New physics in pure and semi tauonic B decays

Ryoutaro Watanabe

New physics in pure and semi tauonic B decays
(タウ粒子を伴う B 中間子崩壊における新物理)

Abstract

Recent experimental results on exclusive semi-tauonic B meson decays, $\bar{B} \to D^{(*)}\tau\bar{\nu}$, show sizable deviations from the standard model prediction, while the recent results on pure-tauonic decay, $\bar{B} \to \tau\bar{\nu}$, reduce the deviation from the prediction. These results suggest a new physics in which the structure of the relevant weak charged interaction may differ from that of the standard model. We study the pure- and semi-tauonic B decays in a model-independent manner using the most general set of four-Fermi interactions in order to clarify possible structures of the charged current in new physics. It turns out that correlations among observables including tau and D^* polarizations and q^2 distributions in $\bar{B} \to D^{(*)}\tau\bar{\nu}$ are useful to distinguish possible new physics operators. Further, we investigate some interesting models to exhibit the advantage of our model-independent analysis. In addition, such model analysis puts constraints on new physics model parameters from the combinations of $\bar{B} \to \tau\bar{\nu}$ and $\bar{B} \to D^{(*)}\tau\bar{\nu}$. As a result, we find that two Higgs doublet models without tree-level FCNC and the minimal supersymmetric standard model with R-parity violation are unlikely to explain the present experimental data, while two Higgs doublet models with FCNC and a leptoquark model are consistent with the data.

Contents

I. INTRODUCTION

The study of nuclear β decays have established the structure of weak interactions for quarks and leptons in the first generation[1]. Following suit with this study, the B factories and LHCb experiments have investigated the counterpart in the second and third generations, and have reported a lot of their results on B meson decays. Since fermions in the second and third generations have large masses, they are crucial keys to understand the mechanism of Electroweak Symmetry Breaking (EWSB). In this respect, they are expected to be relatively more sensitive to new physics unlike the first generation quarks and leptons.

The EWSB sector in a candidate of new physics beyond the standard model (SM) often has a different structure from that of the SM. A well-known example is the two Higgs doublet model (2HDM) of type II [2], which has the Higgs sector identical to that of the minimal supersymmetric standard model (MSSM) [3] at the tree level. A pair of charged Higgs bosons appears in this model, and its couplings to fermions are proportional to the involved fermion masses and further enhanced if the ratio of vacuum expectation values, $\tan\beta$, is large.

Among the B meson decays, $\bar{B} \to \tau\bar{\nu}$ and $\bar{B} \to D^{(*)}\tau\bar{\nu}$ contain both the heavy quark (b) and lepton (τ) in the third generation. Therefore these processes are relatively sensitive to the effect of the charged Higgs bosons[4, 5], while they are described as processes mediated by a W boson in the SM as shown in Fig. 1. From the experimental point of view, these decay processes are rather difficult to be identified because of two or more missing neutrinos in the final states. At (super) B factories, however, reconstructing one of the B mesons in the $e^+e^- \to \Upsilon(4S) \to B\bar{B}$ reaction, one can compare properties of the remaining particles to those expected for signal and background. This method allows us to identify and measure the B meson decays including missing particles. The Belle and BABAR collaborations reported their new results of $\bar{B} \to \tau\bar{\nu}$ and $\bar{B} \to D^{(*)}\tau\bar{\nu}$ respectively in the last year [6, 7] using the full data set, and nowadays these decays get bear watching processes due to their remarkable results shown below.

The pure-tauonic B meson decay $\bar{B} \to \tau\bar{\nu}$ involves the product of the B meson decay constant f_B and the magnitude of the Cabibbo-Kobayashi-Maskawa (CKM) matrix element $|V_{ub}|$ in the SM. Then if we use the value, $f_B = (191 \pm 9)$MeV, determined by the lattice QCD study[8], we obtain $|V_{ub}|$ from this process in the absence of new physics. Before the

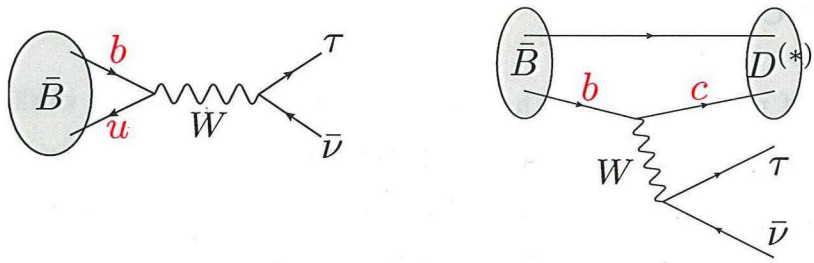

FIG. 1: W boson contribution to the decays.

	$\bar{B} \to \tau\bar{\nu}$ (Belle[6])	$\bar{B} \to \tau\bar{\nu}$ (Average)	CKM fit
$\lvert V_{ub}\rvert \times 10^3$	3.34 ± 0.69	4.21 ± 0.47	3.38 ± 0.15

TABLE I: Determinations of $|V_{ub}|$.

Belle result recently updated, there was some large discrepancy between the values of $|V_{ub}|$ determined by $\bar{B} \to \tau\bar{\nu}$ and the unitarity triangle fit of CKM matrix. This situation seemed to suggest a existence of sizable new physics effect in this process. However, the latest result reported by the Belle collaborations [6] turns out to be consistent with the prediction in the SM (the fit from CKM triangle). In Table I, we summarize the determinations of $|V_{ub}|$, where the average value is obtained by the combination of Belle [6] and BABAR [9] results. The exclusive/inclusive semileptonic decays $B \to \pi\ell\bar{\nu}/B \to X_u\ell\bar{\nu}$ are also used to determine $|V_{ub}|$. However, there is also discrepancy among the values of $|V_{ub}|$ determined from $B \to \pi\ell\bar{\nu}$ and $B \to X_u\ell\bar{\nu}$ beyond the uncertainties that come from hadronic amplitudes [10]. In this thesis, we focus on the deviation between the values from the decay $\bar{B} \to \tau\bar{\nu}$ and the indirect determination by use of the unitarity triangle of CKM matrix.

The semi-tauonic B meson decays $\bar{B} \to D^{(*)}\tau\bar{\nu}$ involve the CKM matrix element $|V_{cb}|$ and the $\bar{B} \to D^{(*)}$ transitions which are well-described by the Heavy quark effective theory (HQET) [11]. The determination of $|V_{cb}|$ is made by using the semileptonic decays $\bar{B} \to D^{(*)}\ell\bar{\nu}$, where ℓ denotes light leptons e or μ. The values determined by these decays are not inconsistent with each other and the determination by inclusive decay [10]. Thus, $\bar{B} \to D^{(*)}\ell\bar{\nu}$ are supposed to be less sensitive to the EWSB sector and assumed to be described by the SM in this thesis. For a precise measurement and prediction of $\bar{B} \to D^{(*)}\tau\bar{\nu}$, it is useful to take the ratio of branching fraction to these light-leptonic decay modes. The

	BABAR[7]	Average	Prediction (SM)
$R(D)$	0.44 ± 0.07	0.42 ± 0.06	0.305 ± 0.012
$R(D^*)$	0.33 ± 0.03	0.34 ± 0.03	0.252 ± 0.004

TABLE II: Measurements and predictions of $R(D^{(*)})$.

ratios of the branching fractions are defined by

$$R(D^{(*)}) \equiv \frac{\mathcal{B}(\bar{B} \to D^{(*)}\tau^-\bar{\nu}_\tau)}{\mathcal{B}(\bar{B} \to D^{(*)}\ell^-\bar{\nu}_\ell)}, \tag{1}$$

and their experimental and predicted values are summarized in Table II, where the average values are obtained by the combination of BABAR [7] and Belle [12–14] assuming the gaussian distribution. (For detail, see in appendix A.) As seen in Table II, the SM is disfavored at 3.5σ and then these results suggest an existence of sizable new physics effects. As shown in Ref.[7], however, one finds that these excesses cannot be explained by a charged Higgs boson in the 2HDM of type II at the same time. It is naively expected that the situation on both the results of $\bar{B} \to D^{(*)}\tau\bar{\nu}$ and $\bar{B} \to \tau\bar{\nu}$ is not suitable for the 2HDM because the result of $\bar{B} \to \tau\bar{\nu}$ is consistent with the prediction in SM as explained above.

Comparing the pure- and semi- tauonic B decays, the latter provides a wide variety of observables besides the branching fraction. Hence, the semi-tauonic processes will allow us to investigate the structure of the relevant charged current interaction at a future B factory. There are many previous studies on such observables [15–29]. Among them we have been investigating the utility for the tau and D^* polarization and shown these quantities are useful to identify the structure of the interaction in these decays [27, 29]. This thesis is mainly based on our these studies.

In addition, we point out that combining the results of $\bar{B} \to \tau\bar{\nu}$ and $\bar{B} \to D^{(*)}\tau\bar{\nu}$ allow us to constrain some classes of new physics models, since these processes often correlate to each other in some new physics models. The 2HDM is a typical example. The suppressed and sizable new physics evidences in pure- and semi- tauonic processes implied by the recent studies are expected to give strong constraints on some of new physics models. Therefore it is useful to take pure- and semi- tauonic decays into account for the sake of new physics effect in the charged current processes.

The rest of this thesis is organized as follows: In Sec. II, we present the most general effective Lagrangian of $b \to q\tau\bar{\nu}$ and the resultant amplitudes of $\bar{B} \to \tau\bar{\nu}$ and $\bar{B} \to D^{(*)}\tau\bar{\nu}$. Experimental constraints are given in Sec. III. We discuss the utilities of the other quantities in the search for new physics in Sec. IV and show the illustration for distinguishing the type of new physics interactions in Sec. V. We analyze 2HDMs, MSSM with R-parity violation and a leptoquark model in Sec. VI. Section VII is devoted to our conclusions.

II. MODEL INDEPENDENT FORMALISM

A. Effective Lagrangian for $b \to q\tau\bar{\nu}$

The bottom quark decay including the tau-lepton, $b \to q\tau\bar{\nu}$, is described by the four-Fermi interaction of charged left-handed currents in the SM. Other four-Fermi operators might be induced in the presence of new physics. The effective Lagrangian that contains all conceivable four-Fermi operators is written as

$$\mathcal{L}_{\rm eff} = -2\sqrt{2}G_F V_{qb}\left((1+C_{V_1}^q)\mathcal{O}_{V_1}^q + C_{V_2}^q\mathcal{O}_{V_2}^q + C_{S_1}^q\mathcal{O}_{S_1}^q + C_{S_2}^q\mathcal{O}_{S_2}^q + C_T^q\mathcal{O}_T^q\right), \tag{2}$$

where the four-Fermi operators are defined by

$$\mathcal{O}_{V_1}^q = \bar{q}_L\gamma^\mu b_L\,\bar{\tau}_L\gamma_\mu(\nu_\tau)_L\,, \tag{3}$$

$$\mathcal{O}_{V_2}^q = \bar{q}_R\gamma^\mu b_R\,\bar{\tau}_L\gamma_\mu(\nu_\tau)_L\,, \tag{4}$$

$$\mathcal{O}_{S_1}^q = \bar{q}_L b_R\,\bar{\tau}_R(\nu_\tau)_L\,, \tag{5}$$

$$\mathcal{O}_{S_2}^q = \bar{q}_R b_L\,\bar{\tau}_R(\nu_\tau)_L\,, \tag{6}$$

$$\mathcal{O}_T^q = \bar{q}_R\sigma^{\mu\nu}b_L\,\bar{\tau}_R\sigma_{\mu\nu}(\nu_\tau)_L\,, \tag{7}$$

and $C_X^q\,(X = V_{1,2}, S_{1,2}, T)$ denotes the Wilson coefficient of $\mathcal{O}_X^q$ as the ratio of the SM contribution. As for the tensor operator, we use the notation: $\sigma^{\mu\nu} = (i/2)\,[\gamma^\mu, \gamma^\nu]$. In later analysis, we also consider the case for the neutrino flavor violating new physics operators $b \to q\tau\bar{\nu}_\ell$, where the neutrino flavor is specified by $\ell = e, \mu$. We take all cases of $\ell = e$, μ and τ into account in the contributions of new physics because the experiment does not identify the neutrino flavor. Since then, the neutrino mixing does not affect the following argument provided that the Pontecorvo-Maki-Nakagawa-Sakata matrix is unitary. Here we assume that the light neutrinos are left-handed. The SM contribution is expressed by the term of 1 in the right hand side of Eq. (2). We see that the tensor operator with the opposite set of quark chiralities $\bar{q}_L\sigma^{\mu\nu}b_R\,\bar{\tau}_R\sigma_{\mu\nu}(\nu_\tau)_L$ identically vanishes, by use of the Fierz transformations,

$$\overline{\psi}_a\Gamma_i\psi_b\,\overline{\psi}_c\Gamma_i\psi_d = -\frac{1}{4}\sum_j F_{ij}\overline{\psi}_a\Gamma_j\psi_d\,\overline{\psi}_c\Gamma_j\psi_b, \tag{8}$$

where $\Gamma = \{1, \gamma^\mu, \sigma^{\mu\nu}/\sqrt{2}, \gamma^\mu\gamma^5, \gamma^5\}$ and

$$F = \begin{pmatrix} 1 & 1 & 1 & 1 & 1 \\ 4 & -2 & 0 & 2 & -4 \\ 6 & 0 & -2 & 0 & 6 \\ 4 & 2 & 0 & -2 & -4 \\ 1 & -1 & 1 & -1 & 1 \end{pmatrix}. \tag{9}$$

B. Decay rate for $\bar{B} \to \tau\bar{\nu}$

The calculation of the two body decay is straightforward. For $\bar{B} \to \tau\bar{\nu}$, defining the B meson decay constant as

$$\langle 0|\bar{u}\gamma^\mu\gamma^5 b|\bar{B}\rangle = f_B p^\mu\,, \tag{10}$$

we obtain the decay rate:

$$\Gamma(\bar{B} \to \tau\bar{\nu}) = \frac{1}{8\pi} G_F^2 |V_{ub}|^2 f_B^2 m_B m_\tau^2 \left(1 - \frac{m_\tau^2}{m_B^2}\right)^2 |1 + r_{\rm NP}|^2\,, \tag{11}$$

where the new physics contributions are summarized into $r_{\rm NP}$ which is represented as

$$r_{\rm NP} = C_{V_1}^u - C_{V_2}^u + \frac{m_B^2}{m_b m_\tau}\left(C_{S_1}^u - C_{S_2}^u\right). \tag{12}$$

We note that the tensor operator $\mathcal{O}_T^u$ does not contribute to the two body decay since the hadronic part $\langle 0|\mathcal{O}_T^u|\bar{B}\rangle$ cannot have anti-symmetric structure of momentum kinematically. As seen in Eq. (12), the type of new physics operator does not much affect the contribution to the decay rate. The enhancement factor $m_B^2/(m_b m_\tau) \sim 3$ in the scalar type contribution is rather small compared to the case for $B_s \to \mu^+\mu^-$.[1] Nevertheless, one finds that $\bar{B} \to \tau\bar{\nu}$ are the most sensitive to the scalar interactions among the decays related to $b \to q\tau\bar{\nu}$ due to the pseudo scalar meson $\bar{B}$ and its two body decay.

C. Helicity amplitudes for $\bar{B} \to D^{(*)}\tau\bar{\nu}$

The helicity amplitude of $\bar{B} \to M\tau\bar{\nu}\,(M = D, D^*)$ is written as

$$\mathcal{M}^{\lambda_\tau,\lambda_M} = \mathcal{M}_{\rm SM}^{\lambda_\tau,\lambda_M} + \mathcal{M}_{V_1}^{\lambda_\tau,\lambda_M} + \mathcal{M}_{V_2}^{\lambda_\tau,\lambda_M} + \mathcal{M}_{S_1}^{\lambda_\tau,\lambda_M} + \mathcal{M}_{S_2}^{\lambda_\tau,\lambda_M} + \mathcal{M}_T^{\lambda_\tau,\lambda_M}\,, \tag{13}$$

[1] In this case, the scalar interaction is enhanced by the factor $m_B^2/(m_b m_\mu) \sim 60$. For detail, see Ref. [39].

where λ_τ is the helicity of the tau lepton, $\lambda_M = s$ indicates the amplitude of $\bar{B} \to D\tau\bar{\nu}$, and $\lambda_M = \pm 1, 0$ denotes the D^* helicity defined in the B rest frame. The amplitude $\mathcal{M}_{\rm SM}^{\lambda_\tau,\lambda_M}$ represents the SM contribution and other terms in the right-hand side stand for new physics contributions corresponding to the operators in Eqs. (3)–(7). The SM amplitude is given by [30, 31]

$$\mathcal{M}_{\rm SM}^{\lambda_\tau,\lambda_M} = \frac{G_F}{\sqrt{2}} V_{cb} \sum_\lambda \eta_\lambda H_{V_1,\lambda}^{\lambda_M} L_{\lambda,\tau}^{\lambda_\tau}\,, \tag{14}$$

and the amplitudes that represent new physics contributions take the following forms:

$$\mathcal{M}_{V_i}^{\lambda_\tau,\lambda_M} = \frac{G_F}{\sqrt{2}} V_{cb} C_{V_i}^c \sum_\lambda \eta_\lambda H_{V_i,\lambda}^{\lambda_M} L_\lambda^{\lambda_\tau} \quad (i = 1, 2)\,, \tag{15}$$

$$\mathcal{M}_{S_i}^{\lambda_\tau,\lambda_M} = -\frac{G_F}{\sqrt{2}} V_{cb} C_{S_i}^c H_{S_i}^{\lambda_M} L^{\lambda_\tau} \quad (i = 1, 2)\,, \tag{16}$$

$$\mathcal{M}_T^{\lambda_\tau,\lambda_M} = -\frac{G_F}{\sqrt{2}} V_{cb} C_T^c \sum_{\lambda,\lambda'} \eta_\lambda \eta_{\lambda'} H_{\lambda\lambda'}^{\lambda_M} L_{\lambda\lambda'}^{\lambda_\tau}\,, \tag{17}$$

where H's and L's are the hadronic and leptonic amplitudes respectively as defined below; $\lambda, \lambda' = \pm, 0, s$ denote the virtual vector boson helicity. The metric factor η_λ is given by $\eta_{\pm,0} = 1$ and $\eta_s = -1$. We treat the contraction of the Lorentz indices in $\mathcal{O}_T^c$ as if two heavy vector bosons are exchanged.

The leptonic amplitudes, $L_\lambda^{\lambda_\tau}$, L^{λ_τ} and $L_{\lambda\lambda'}^{\lambda_\tau}$ are defined by

$$L_\lambda^{\lambda_\tau}(q^2, \cos\theta_\tau) = \epsilon_\mu(\lambda) \langle \tau(p_\tau, \lambda_\tau) \bar{\nu}_\tau(p_\nu) | \bar{\tau} \gamma^\mu (1 - \gamma_5) \nu_\tau | 0 \rangle\,, \tag{18}$$

$$L^{\lambda_\tau}(q^2, \cos\theta_\tau) = \langle \tau(p_\tau, \lambda_\tau) \bar{\nu}_\tau(p_\nu) | \bar{\tau} (1 - \gamma_5) \nu_\tau | 0 \rangle\,, \tag{19}$$

$$L_{\lambda\lambda'}^{\lambda_\tau}(q^2, \cos\theta_\tau) = -i \epsilon_\mu(\lambda) \epsilon_\nu(\lambda') \langle \tau(p_\tau, \lambda_\tau) \bar{\nu}_\tau(p_\nu) | \bar{\tau} \sigma^{\mu\nu} (1 - \gamma_5) \nu_\tau | 0 \rangle\,, \tag{20}$$

where $\epsilon_\mu(\lambda)$ represents the polarization vector of the virtual vector boson, $q^\mu = p_B^\mu - p_M^\mu (= p_\tau^\mu + p_\nu^\mu)$ is the momentum transfer, and θ_τ denotes the angle between the momentum of the tau lepton and that of the M meson in the rest frame of the leptonic system, to which we refer as the q rest frame. The τ helicity λ_τ is also defined in the q rest frame. The explicit

formulae of the leptonic amplitudes for vector type operators are given by

$$L_{\pm}^{+} = \pm\sqrt{2}m_\tau v \sin\theta_\tau \ , \tag{21}$$

$$L_{0}^{+} = 2m_\tau v \cos\theta_\tau \ , \tag{22}$$

$$L_{s}^{+} = -2m_\tau v \ , \tag{23}$$

$$L_{\pm}^{-} = \sqrt{2}\sqrt{q^2}v(1 \pm \cos\theta_\tau) \ , \tag{24}$$

$$L_{0}^{-} = -2\sqrt{q^2}v \sin\theta_\tau \ , \tag{25}$$

$$L_{s}^{-} = 0 \ , \tag{26}$$

where $v = \sqrt{1 - m_\tau^2/q^2}$. The scalar type leptonic amplitudes are written as

$$L^{+} = -2\sqrt{q^2}v \ , \tag{27}$$

$$L^{-} = 0 \ . \tag{28}$$

The tensor type leptonic amplitudes are represented as

$$L_{\lambda\lambda}^{\pm} = 0 \ , \tag{29}$$

$$L_{0\pm}^{+} = -L_{\pm 0}^{+} = -\sqrt{2}\sqrt{q^2}v \sin\theta_\tau \ , \tag{30}$$

$$L_{+-}^{+} = -L_{-+}^{+} = L_{s0}^{+} = -L_{0s}^{+} = 2\sqrt{q^2}v \cos\theta_\tau \ , \tag{31}$$

$$L_{\pm s}^{+} = -L_{s\pm}^{+} = \mp\sqrt{2}\sqrt{q^2}v \sin\theta_\tau \ , \tag{32}$$

$$L_{0\pm}^{-} = -L_{\pm 0}^{-} = \mp\sqrt{2}m_\tau v(1 \pm \cos\theta_\tau) \ , \tag{33}$$

$$L_{+-}^{-} = -L_{-+}^{-} = L_{s0}^{-} = -L_{0s}^{-} = -2m_\tau v \sin\theta_\tau \ , \tag{34}$$

$$L_{\pm s}^{-} = -L_{s\pm}^{-} = -\sqrt{2}m_\tau v(1 \pm \cos\theta_\tau) \ . \tag{35}$$

The formulae of the lepton amplitudes for different neutrino flavor are the same as the above results as long as the mass of neutrino is very small and ignored.

The hadronic amplitudes, $H_{V_i,\lambda}^{\lambda_M}$, $H_{S_i}^{\lambda_M}$ and $H_{\lambda\lambda'}^{\lambda_M}$ are defined by

$$H_{V_1,\lambda}^{\lambda_M}(q^2) = \epsilon_\mu^*(\lambda)\langle M(p_M, \epsilon(\lambda_M))\,|\bar{c}\gamma^\mu(1-\gamma^5)b|\bar{B}(p_B)\rangle \ , \tag{36}$$

$$H_{V_2,\lambda}^{\lambda_M}(q^2) = \epsilon_\mu^*(\lambda)\langle M(p_M, \epsilon(\lambda_M))\,|\bar{c}\gamma^\mu(1+\gamma^5)b|\bar{B}(p_B)\rangle \ , \tag{37}$$

$$H_{S_1}^{\lambda_M}(q^2) = \langle M(p_M, \epsilon(\lambda_M))\,|\bar{c}(1+\gamma^5)b|\bar{B}(p_B)\rangle \ , \tag{38}$$

$$H_{S_2}^{\lambda_M}(q^2) = \langle M(p_M, \epsilon(\lambda_M))\,|\bar{c}(1-\gamma^5)b|\bar{B}(p_B)\rangle \ , \tag{39}$$

$$H_{\lambda\lambda'}^{\lambda_M}(q^2) = i\epsilon_\mu^*(\lambda)\epsilon_\nu^*(\lambda')\langle M(p_M, \epsilon(\lambda_M))\,|\bar{c}\sigma^{\mu\nu}(1-\gamma^5)b|\bar{B}(p_B)\rangle, \tag{40}$$

where $\epsilon(\lambda_M)$ denotes the polarization vector of D^* for $\lambda_M = \pm 1, 0$. The relations $H^s_{V_1,\lambda} = H^s_{V_2,\lambda}$ and $H^s_{S_1} = H^s_{S_2}$ hold because of the parity conservation in the strong interaction. Similarly, we find $H^{\lambda_M}_{S_1} = -H^{\lambda_M}_{S_2}$ for $\lambda_M = \pm 1, 0$. The hadronic amplitudes of the vector type operators for $\bar{B} \to D\tau\bar{\nu}$ defined in Eqs. (36) and (37) are represented as

$$H^s_{V_1,\pm}(q^2) = H^s_{V_2,\pm}(q^2) = 0\,, \tag{41}$$

$$H^s_{V_1,0}(q^2) = H^s_{V_2,0}(q^2) = m_B\sqrt{r}(1+r)\frac{\sqrt{w^2-1}}{\sqrt{\hat{q}^2(w)}}\,V_1(w)\,, \tag{42}$$

$$H^s_{V_1,s}(q^2) = H^s_{V_2,s}(q^2) = m_B\sqrt{r}(1-r)\frac{w+1}{\sqrt{\hat{q}^2(w)}}\,S_1(w)\,, \tag{43}$$

and those for $\bar{B} \to D^*\tau\bar{\nu}$ are

$$H^{\pm}_{V_1,\pm}(q^2) = -H^{\mp}_{V_2,\mp}(q^2) = m_B\sqrt{r}A_1(w)\left[w+1\mp\sqrt{w^2-1}R_1(w)\right]\,, \tag{44}$$

$$H^0_{V_1,0}(q^2) = -H^0_{V_2,0}(q^2) = m_B\sqrt{r}\frac{w+1}{\sqrt{\hat{q}^2(w)}}A_1(w)\left[-w+r+(w-1)R_2(w)\right]\,, \tag{45}$$

$$\begin{aligned} H^0_{V_1,s}(q^2) &= -H^0_{V_2,s}(q^2) \\ &= \frac{m_B}{2\sqrt{r}}\frac{\sqrt{w^2-1}}{\sqrt{\hat{q}^2(w)}}A_1(w)\left[-2r(w+1)+(1-r^2)R_2(w)-\hat{q}^2(w)R_3(w)\right]\,, \end{aligned} \tag{46}$$

$$\text{others} = 0, \tag{47}$$

where $\hat{q}^2(w) = 1+r^2-2rw$, $r = m_M/m_B$, and $w = p_B\cdot p_M/(m_B m_M)$ is the velocity transfer in $\bar{B} \to M\tau\bar{\nu}$. The form factors, $V_1(w), S_1(w), A_1(w)$ and $R_i(w)$ are defined in Appendix D. The amplitudes of the scalar type operators are expressed in terms of vector form factors by applying the equations of motion of the quark fields:

$$H^s_{S_1}(q^2) = H^s_{S_2}(q^2) = m_B\sqrt{r}(w+1)S_1(w)\,, \tag{48}$$

$$H^{\pm}_{S_1}(q^2) = H^{\pm}_{S_2}(q^2) = 0\,, \tag{49}$$

$$\begin{aligned} H^0_{S_1}(q^2) &= -H^0_{S_2}(q^2) \\ &= \frac{m_B\sqrt{w^2-1}}{2\sqrt{r}(1+r)}A_1(w)\left[-2r(w+1)+(1-r^2)R_2(w)-\hat{q}^2(w)R_3(w)\right]\,. \end{aligned} \tag{50}$$

Similarly, for the tensor operator, we obtain

$$H^s_{+-}(q^2) = H^s_{0s}(q^2) = m_B\sqrt{r}\frac{\sqrt{w^2-1}}{\hat{q}^2(w)}[-(1+r)^2 V_1(w) + 2r(w+1)S_1(w)], \quad (51)$$

$$H^{\pm}_{\pm 0}(q^2) = \pm H^{\pm}_{\pm s}(q^2)$$
$$= \frac{m_B\sqrt{r}}{\sqrt{\hat{q}^2(w)}}A_1(w)\left[\pm(1-r)(w+1) + (1+r)\sqrt{w^2-1}R_1(w)\right], \quad (52)$$

$$H^0_{+-}(q^2) = H^0_{0s}(q^2)$$
$$= \frac{m_B\sqrt{r}}{1+r}A_1(w)\left[-(w+r)(w+1) + (w^2-1)R_3(w)\right], \quad (53)$$

$$H^{\lambda_M}_{\lambda\lambda'}(q^2) = -H^{\lambda_M}_{\lambda'\lambda}(q^2), \quad (54)$$

and others $= 0$. A definitions of form factors and a detailed derivation of these hadronic amplitudes are found in Appendix B and Appendix D respectively.

The differential decay rate $\bar{B} \to M\tau\bar{\nu}$ is represented as

$$d\Gamma^{\lambda_\tau}_{\lambda_M} = \frac{1}{2m_B}\left|\mathcal{M}^{\lambda_\tau,\lambda_M}(q^2,\cos\theta_\tau)\right|^2 d\Phi_3, \quad (55)$$

where the three-body phase space $d\Phi_3$ is given by

$$d\Phi_3 = \frac{\sqrt{Q_+Q_-}}{256\pi^3 m_B^2}\left(1-\frac{m_\tau^2}{q^2}\right)dq^2 d\cos\theta_\tau, \quad (56)$$

and $Q_\pm = (m_B \pm m_M)^2 - q^2$. Several decay rates used in the main text are obtained by integrating Eq. (55) over q^2 and $\cos\theta_\tau$. For notational simplicity, we define the following quantities:

$$\Gamma^{\pm}(D) = \Gamma^{\pm 1/2}_s, \quad \Gamma^{\pm}(D^*) = \sum_{\lambda_M=\pm1,0}\Gamma^{\pm 1/2}_{\lambda_M}, \quad (57)$$

$$\Gamma(D^*_T) = \sum_{\lambda_M=\pm1}\sum_{\lambda_\tau}\Gamma^{\lambda_\tau}_{\lambda_M}, \quad \Gamma(D^*_L) = \sum_{\lambda_\tau}\Gamma^{\lambda_\tau}_0. \quad (58)$$

We note that the angle θ_τ (which has been defined as the angle between the momentum of the tau lepton and that of the M meson in the q rest frame) cannot be measured since we generally do not know the tau momentum. However, it is in principle (at least) possible to measure the direction of the tau remaining two-fold ambiguity if we know the position of the $\bar{B}$ and τ decay point using the decay vertex detector, which will be an additional improvement of a super B factory. It is important to investigate an utility of such an information in preparation for a super B factory, but this is beyond our work for now.[2]

[2] The LHCb collaboration recently begun to analyze $\bar{B} \to D^*\tau\bar{\nu}$ using such a method.

D. CKM matrix element, form factors and SM predictions

Precise determinations of $|V_{ub}|$ and $|V_{cb}|$ are important issues to not only confirm the CKM sector of the SM but also search for new physics in $b \to u, c$ transitions. This also require the correct estimations (or predictions) of hadronic amplitudes.

1. $\bar{B} \to D^{(*)}\ell\bar{\nu}$

Here, we briefly review the recent determinations of $|V_{cb}|$ in $\bar{B} \to D^{(*)}\ell\bar{\nu}$ and the estimations of their hadronic amplitudes. Using the helicity amplitudes shown in Eqs.(21)–(26) and (41)–(47), and replacing $m_\tau \to m_\ell \simeq 0$, the differential decay rates in $\bar{B} \to D\ell\bar{\nu}$ and $\bar{B} \to D^*\ell\bar{\nu}$ are given by

$$\frac{d\Gamma}{dw}(\bar{B} \to D\ell\bar{\nu}) = \frac{G_F|V_{cb}|^2 m_B^5}{48\pi^3} r^3 (1+r)^2 (w^2-1)^{3/2} \mathcal{F}_D(w)^2, \tag{59}$$

$$\frac{d\Gamma}{dw}(\bar{B} \to D^*\ell\bar{\nu}) = \frac{G_F|V_{cb}|^2 m_B^5}{48\pi^3} r^3 \sqrt{w^2-1}(w+1)^2 P(w) \mathcal{F}_{D^*}(w)^2, \tag{60}$$

in the SM, where

$$P(w) = (1-r)^2 + \frac{4w}{w+1}\hat{q}^2(w), \tag{61}$$

and $\mathcal{F}$'s indicate the contributions of the form factors represented as

$$\mathcal{F}_D(w) = V_1(w), \tag{62}$$

$$\mathcal{F}_{D^*}(w) = A_1(w)\left[2\hat{q}^2(w)\left(1 + \frac{w-1}{w+1}R_1(w)\right)\right. \tag{63}$$

$$\left. + [1 - r + (w-1)(1 - R_2(w))]^2\right]^{1/2} / \sqrt{P(w)}. \tag{64}$$

In the framework of the HQET, one finds $\mathcal{F}_D(w) = \mathcal{F}_{D^*}(w) = \xi(w)$ in the heavy quark limit, where $\xi(w)$ is called as the (leading) Isgur-Wise function [32]. Containing $1/m_Q$ corrections, the three additional undetermined functions $\chi_{2,3}$ and η_3, which are referred as sub-leading Isgur-Wise functions, appear in $\bar{B} \to D^{(*)}\ell\bar{\nu}$. We briefly review the HQET and show the detailed expressions for the form factors including $1/m_Q$ corrections in Appendix. C. Luke's theorem [33] implies that the $1/m_Q$ corrections disappear at the zero recoil limit $w \to 1$.

Thus, the absence of $1/m_Q$ corrections to the hadronic amplitudes reduce the theoretical uncertainties, while we need the extrapolations of the distributions for $\bar{B} \to D^{(*)}\ell\bar{\nu}$, since

the distributions vanish at $w \to 1$ as seen in Eqs. (59) and (60). For the extrapolations, one usually employs the following ansatz [34],

$$V_1(w) = V_1(1)\left[1 - 8\rho_1^2 z + (51.\rho_1^2 - 10.)z^2 - (252.\rho_1^2 - 84.)z^3\right], \tag{65}$$

$$A_1(w) = A_1(1)\left[1 - 8\rho_{A_1}^2 z + (53\rho_{A_1}^2 - 15)z^2 - (231\rho_{A_1}^2 - 91)z^3\right], \tag{66}$$

where $z = (\sqrt{w+1} - \sqrt{2})/(\sqrt{w+1} + \sqrt{2})$ and $R_1(1)$ and $R_2(1)$ are left as fitting parameters. Based on these parameterizations, extrapolations and global fits from the experimental data of the distributions result in [35]

$$\mathcal{F}_D(1)|V_{cb}| = (4.26 \pm 0.07 \pm 0.14) \times 10^{-2}, \tag{67}$$

$$\rho_1^2 = 1.186 \pm 0.055, \tag{68}$$

for $\bar{B} \to D\ell\bar{\nu}$, and

$$\mathcal{F}_{D^*}(1)|V_{cb}| = (3.59 \pm 0.01 \pm 0.04) \times 10^{-2}, \tag{69}$$

$$\rho_{A_1}^2 = 1.207 \pm 0.026, \tag{70}$$

$$R_1(1) = 1.403 \pm 0.033, \tag{71}$$

$$R_2(1) = 0.854 \pm 0.020, \tag{72}$$

for $\bar{B} \to D^*\ell\bar{\nu}$. We cannot determine the overall factors $\mathcal{F}_{D^{(*)}}(1)$ (or equivalently $V_1(1)$ and $A_1(1)$) from the experimental data but can predict from the lattice studies which give $\mathcal{F}_D(1) = 1.074 \pm 0.024$ and $\mathcal{F}_{D^*}(1) = 0.902 \pm 0.017$ [10]. Finally we obtain

$$|V_{cb}| = (3.94 \pm 0.14 \pm 0.13) \times 10^{-2} \quad (\text{from } \bar{B} \to D\ell\bar{\nu}), \tag{73}$$

$$|V_{cb}| = (3.96 \pm 0.06 \pm 0.08) \times 10^{-2} \quad (\text{from } \bar{B} \to D^*\ell\bar{\nu}). \tag{74}$$

These values are quite consistent with each other.

2. $\bar{B} \to D^{(*)}\tau\bar{\nu}$

The amplitude in $\bar{B} \to D\tau\bar{\nu}$ involves two distinct form factors, $V_1(w)$ and $S_1(w)$. The form factor $S_1(w)$ does not contribute to $\bar{B} \to D\ell\bar{\nu}$ as seen above. In order to see new physics effect in $\bar{B} \to D\tau\bar{\nu}$, we have to estimate $S_1(w)$ without experimental data. Applying the

HQET to the form factors, one find that $S_1(w)$ and $V_1(w)$ reduce to the Isgur-Wise function in the heavy quark limit. Accordingly we parameterize it as

$$S_1(w) = [1 + \Delta(w)]\, V_1(w)\,, \tag{75}$$

where $\Delta(w)$ denotes the QCD and $1/m_Q$ corrections. As shown in Appendix D, we estimate $\Delta(w)$ and give an approximate formula [29]:

$$\Delta(w) = -0.019 + 0.041(w-1) - 0.015(w-1)^2\,. \tag{76}$$

As for $\bar{B} \to D^*\tau\bar{\nu}$, four form factors, $A_1(w)$ and $R_{1,2,3}(w)$, contribute. The w dependence of $A_1(w)$ and the zero recoil limit of $R_{1,2}(1)$ are extracted from experimental data of $\bar{B} \to D^*\ell\bar{\nu}$. The w dependence of $R_{1,2}(w)$ is estimated by the HQET, while the leading terms $R_1(1)$ and $R_2(1)$ are left as fitting parameters determined above:

$$R_1(w) = R_1(1) - 0.12(w-1) + 0.05(w-1)^2\,, \tag{77}$$

$$R_2(w) = R_2(1) + 0.11(w-1) - 0.06(w-1)^2\,. \tag{78}$$

The form factor $R_3(w)$ appears only in $\bar{B} \to D^*\tau\bar{\nu}$ and is estimated as [27]

$$R_3(w) = 1 + \Delta_3(w), \quad \Delta_3(w) = 0.22 - 0.052(w-1) + 0.026(w-1)^2\,. \tag{79}$$

The derivations of $R_{1,2,3}(w)$ using the HQET are shown in Appendix D.

The decay rates of $\bar{B} \to D^{(*)}\tau\bar{\nu}$ are then predicted by use of the parameters determined from $\bar{B} \to D^{(*)}\ell\bar{\nu}$ and predicted from the HQET. Taking the ratio of the decay rates $\bar{B} \to D^{(*)}\tau\bar{\nu}$ to the semileptonic decays $\bar{B} \to D^{(*)}\ell\bar{\nu}$ further reduces the theoretical and experimental uncertainties which mainly come from $\mathcal{F}_{D^{(*)}}(1)|V_{cb}|$. We define the ratios as

$$R(D^{(*)}) = \frac{\Gamma^+(D^{(*)}) + \Gamma^-(D^{(*)})}{\Gamma(\bar{B} \to D^{(*)}\ell\bar{\nu})}\,, \tag{80}$$

where $\Gamma^{\pm}(D^{(*)})$ are defined in Eq. (57) and $\Gamma(\bar{B} \to D^{(*)}\ell\bar{\nu})$ are obtained by integrating Eqs. (59) and (60). The SM predictions and the measured values of $R(D^{(*)})$ are summarized in Table II. Combining the excesses of the measurements give 3.5σ deviation from the SM. These results seem to imply that the sizable new physics effect contribute to $\bar{B} \to D^{(*)}\tau\bar{\nu}$.

3. *Determinations of* $|V_{ub}|$

Here in turn, we shortly review the determinations of $|V_{ub}|$. The semileptonic transition $b \to u\ell\bar{\nu}$ provides two avenues for determining $|V_{ub}|$, that is, the extractions via inclusive and exclusive decays.

The theoretical description of inclusive decay $\bar{B} \to X_u\ell\bar{\nu}$ is based on the HQET. Although the total decay rate is theoretically predicted with uncertainties below 5%, it is hard to measure the total decay rate by experiment because of the large background from $\bar{B} \to X_c\ell\bar{\nu}$. Instead, the partial decay rate in regions, where the rate of $\bar{B} \to X_c\ell\bar{\nu}$ is suppressed, is used to extract $|V_{ub}|$. There are several models to estimate the shape of the distribution and their results of $|V_{ub}|$ are consistent with each other. The Particle Data Group [10] has reported the arithmetic means of their values and errors:

$$|V_{ub}| = (4.41 \pm 0.15 \pm 0.16) \times 10^{-3} \quad (\text{from } \bar{B} \to X_u\ell\bar{\nu}). \tag{81}$$

Determination from exclusive decay is needed as a complemental check for that from inclusive decay $\bar{B} \to X_u\ell\bar{\nu}$ as shown above. For experiment, the identification of the final meson provides better background rejection at the cost of the lower branching fraction, which might be a crucial difficulty for $b \to u$ transition due to doubly Cabibbo suppressed process. For now, the decay $\bar{B} \to \pi\ell\bar{\nu}$ yields the most precise value of $|V_{ub}|$ among exclusive decays. The relevant form factors for $\bar{B} \to \pi\ell\bar{\nu}$ are calculated by the lattice QCD and light-cone sum rules depending on the regions of momentum transfer. We omit the detail here and for detail, see in Ref. [36]. As a result, the recent values of $|V_{ub}|$ from $\bar{B} \to \pi\ell\bar{\nu}$ are averaged as [10]

$$|V_{ub}| = (3.23 \pm 0.31) \times 10^{-3} \quad (\text{from } \bar{B} \to \pi\ell\bar{\nu}). \tag{82}$$

Most of contributions to the uncertainty come from lattice systematic and statistical errors.

As we have shown in Eq. (81) and (82), the deviation between the values of $|V_{ub}|$ reaches 3σ. Therefore we cannot confirm the correct value of $|V_{ub}|$ in the studies of the determinations from the inclusive and exclusive decay processes. Instead, we can predict $|V_{ub}|$ indirectly by use of the unitarity triangle of the CKM matrix. In terms of the Wolfenstein parameters, V_{ub} is parametrized as $V_{ub} = A\lambda^3(\rho - i\eta)$, where $A = 0.811 \pm 0.017$ and $\lambda = 0.225 \pm 0.001$ [10]. What is needed for this approach is the measured values of ρ and η without an information

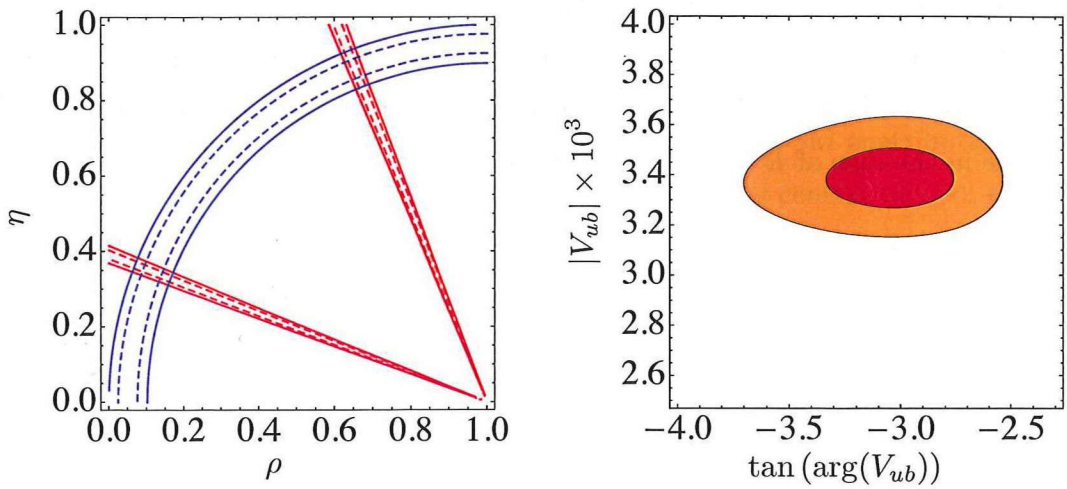

FIG. 2: Left: allowed regions that come from the experimental results of $\tan\phi_1$ (red) and $\Delta m_{B_d}/\Delta m_{B_s}$ (blue) in the ρ–η plane. Right: a prediction of V_{ub} from the fit to the ρ–η plane within 1σ deviation (red region) and 2σ deviation (orange region).

from V_{ub}. This is done by measuring the angle ϕ_1, which is parametrized as

$$\tan\phi_1 = \frac{\eta}{1-\rho}, \tag{83}$$

and the length of the side of the unitarity triangle opposite the angle ϕ_3, that is given by the ratio of B_d–$\bar{B}_d$ and B_s–$\bar{B}_s$ mixing and parametrized as

$$\frac{\Delta m_{B_d}}{\Delta m_{B_s}} = \frac{m_{B_d}}{m_{B_s}} \xi^{-2} \lambda^2 \left((1-\rho)^2 + \eta^2 \right), \tag{84}$$

where $\xi = 1.26 \pm 0.03 \pm 0.02$ [37]. In the left panel of Fig. 2, we show the allowed regions that come from the experimental results of $\tan\phi_1$ (red) and $\Delta m_{B_d}/\Delta m_{B_s}$ (blue) in the ρ–η plane. The measured values we used here are summarized in Ref. [38]. In the right panel, we show the indirect allowed region of V_{ub} from the fit to the values of ρ and η. The vertical axis indicates the absolute value of V_{ub}, which is parametrized as $|V_{ub}| = A\lambda^3\sqrt{\rho^2+\eta^2}$, and the horizontal axis represents the phase, $\tan(\arg(V_{ub})) = -\eta/\rho$. In this work, we treat the value in this region as a reference value of V_{ub}. (This is equivalent to the value in Table I.)

4. $\bar{B} \to \tau\bar{\nu}$

The hadronic contribution to the decay $\bar{B} \to \tau\bar{\nu}$ is summarized into the B meson decay constant f_B, which is calculated as $f_B = (191 \pm 9)$MeV by the lattice QCD study[8]. In the

absence of new physics ($r_{\rm NP} = 0$ in Eq. (12)), thus we can extract $|V_{ub}|$ from the measurement of $\bar{B} \to \tau\bar{\nu}$. In Table I, we show the results, which are consistent with the predicted value from the unitarity of CKM matrix. This mean that the new physics effect is suppressed in $\bar{B} \to \tau\bar{\nu}$ unlike in the case of $\bar{B} \to D^{(*)}\tau\bar{\nu}$ as shown above.

III. EXPERIMENTAL CONSTRAINTS

Let us consider first the constraint on the new physics effect from the measurement of $\bar{B} \to \tau\bar{\nu}$. We defined the Wilson coefficients as a ratio of the SM contribution $(2\sqrt{2}G_F V_{ub})$ in Sec. II. In the following analysis of $\bar{B} \to \tau\bar{\nu}$, we choose the central value of V_{ub} determined by the unitarity of CKM matrix as shown in Table I. We take the world average of $\mathcal{B}(\bar{B} \to \tau\bar{\nu}) = (1.14 \pm 0.23) \times 10^{-4}$ as the measured quantity. Then we find that the constraint on $r_{\rm NP}$ turn out to be

$$|1 + r_{\rm NP}|^2 = 1.53 \pm 0.28. \tag{85}$$

One can see that the deviation is 1.7σ and then $r_{\rm NP} = 0$ is not inconsistent with the measurement for now. This result implies the new physics effect is suppressed in $\bar{B} \to \tau\bar{\nu}$. Then more precise measurement is favorable for the new physics search.

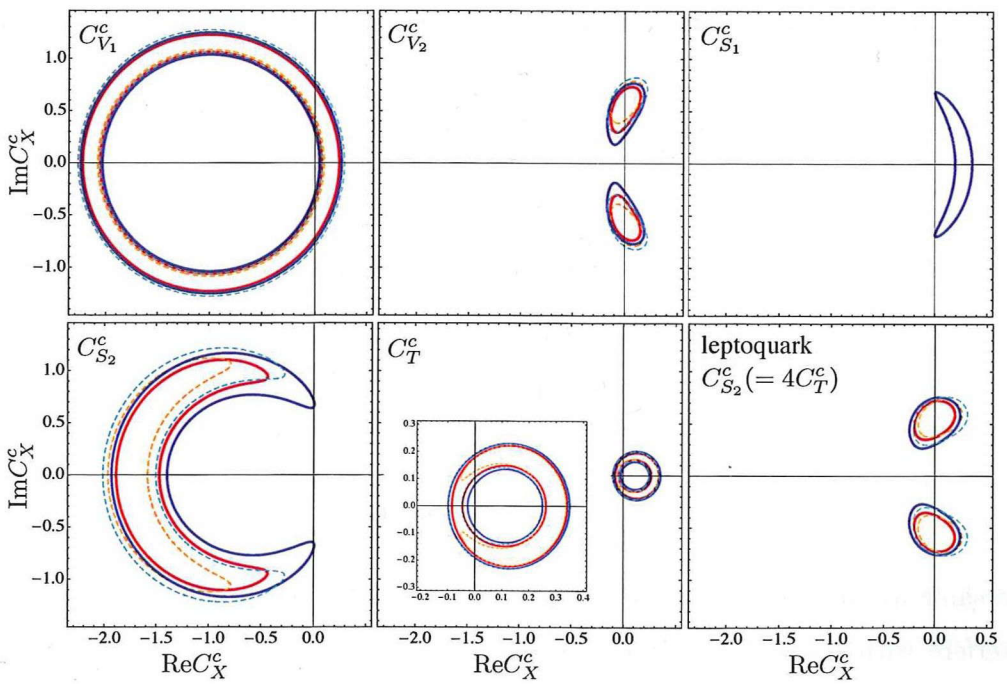

FIG. 3: Constraints on the Wilson coefficient C^c_X. The allowed regions within 95%(red line and orange dashed line) and 99%(blue line and cyan dashed line) CL are shown. The regions in the line (dashed line) are allowed when the values of $R(D^{(*)})$ are evaluated so as to be maximized (minimized) within the hadronic errors. Allowed regions for $|C^{c\nu_\ell}_X|$ are obtained by those for pure imaginary C^c_X. The leptoquark panel is mentioned in Sec. VI.

Next we consider the constraints from $\bar{B} \to D^{(*)}\tau\bar{\nu}$. Unlike the case of $\bar{B} \to \tau\bar{\nu}$, the contribution of the new physics varies depending on the type of new physics operator. In the following model-independent analysis of $\bar{B} \to D^{(*)}\tau\bar{\nu}$, we assume that one of the new physics operators in Eq. (2) is dominant except the SM contribution. This assumption allows us to determine the dominant Wilson coefficient from the experimental results of $R(D)$ and $R(D^*)$, and to see the feature of the contribution of new physics operator. It is also useful to predict other observables as shown later. A situation beyond this assumption is discussed in Sec. VI. In Fig. 3, the allowed region of the complex Wilson coefficient C_X^c is shown for each operator $\mathcal{O}_X^c$. The regions in the line (dashed line) are allowed when the values of $R(D^{(*)})$ are evaluated so as to be maximized (minimized) within the hadronic errors. The vector operators $\mathcal{O}_{V_{1,2}}^c$ describe the current experimental results [40]. The scalar operator $\mathcal{O}_{S_1}^c$ cannot satisfy the current experimental bounds. While the operator $\mathcal{O}_{S_2}^c$ is favored but need a large Wilson coefficient $C_{S_2}^c$ for describing the experimental data, as is already pointed out in Ref. [40, 41]. In addition, we find that the tensor operator $\mathcal{O}_T^c$ reasonably explains the current data.

We can translate these results into the cases of neutrino flavor violating operators. The effects of such operators $\mathcal{O}_X^{c\nu_\ell}$, defined as

$$\mathcal{O}_{V_1}^{c\nu_\ell} = \bar{c}_L\gamma^\mu b_L\,\bar{\tau}_L\gamma_\mu(\nu_\ell)_L\,, \tag{86}$$

$$\mathcal{O}_{V_2}^{c\nu_\ell} = \bar{c}_R\gamma^\mu b_R\,\bar{\tau}_L\gamma_\mu(\nu_\ell)_L\,, \tag{87}$$

$$\mathcal{O}_{S_1}^{c\nu_\ell} = \bar{c}_L b_R\,\bar{\tau}_R(\nu_\ell)_L\,, \tag{88}$$

$$\mathcal{O}_{S_2}^{c\nu_\ell} = \bar{c}_R b_L\,\bar{\tau}_R(\nu_\ell)_L\,, \tag{89}$$

$$\mathcal{O}_T^{c\nu_\ell} = \bar{c}_R\sigma^{\mu\nu} b_L\,\bar{\tau}_R\sigma_{\mu\nu}(\nu_\ell)_L\,, \tag{90}$$

are the same as those of $\mathcal{O}_X^c$ with $\mathrm{Re}C_X^c = 0$, because the new physics contributions do not interfere with the SM amplitudes in these cases. Thus, we find no allowed region of the Wilson coefficient within 99% confidence level (CL) for $\mathcal{O}_{S_1}^{c\nu_\ell}$ nor $\mathcal{O}_{S_2}^{c\nu_\ell}$. The operators $\mathcal{O}_{V_1}^{c\nu_\ell}$, $\mathcal{O}_{V_2}^{c\nu_\ell}$ and $\mathcal{O}_T^{c\nu_\ell}$ are able to explain the present data.

IV. THEORETICAL PREDICTIONS

A. Polarizations

There are several measurable quantities affected by new physics operators in $\bar{B} \to D^{(*)}\tau\bar{\nu}$ even though more than two particles are missing in the final state. In this work, we consider the tau longitudinal polarization[3] in $\bar{B} \to D\tau\bar{\nu}$ and define the following quantity:

$$P_\tau(D) = \frac{\Gamma^+(D) - \Gamma^-(D)}{\Gamma^+(D) + \Gamma^-(D)}, \tag{91}$$

where $\Gamma^\pm(D)$ represents the decay rate with $\lambda_\tau = \pm 1/2$ as defined in Eq. (57). The uncertainties that come from V_{cb} and the normalization factor $V_1(1)$ vanish in the above quantity. For $\bar{B} \to D^*\tau\bar{\nu}$ we also define $P_\tau(D^*)$ in the same fashion. In addition we introduce the D^* polarization as

$$P_{D^*} = \frac{\Gamma(D^*_L)}{\Gamma(D^*_L) + \Gamma(D^*_T)}, \tag{92}$$

where $D^*_{L(T)}$ represents the longitudinally (transversely) polarized D^* and $\Gamma(D^*_{L,T})$ are defined in Eq. (58). The uncertainties in $P_\tau(D^*)$ and P_{D^*} due to V_{cb} and $A_1(1)$ also disappear. The new physics operators are expected to affect these observables in various ways. Thus it is important to study them at the same time in order to distinguish the underlying new physics. Besides the above integrated quantities, q^2 distributions are potentially sensitive to new physics. As we will illustrate below, the q^2 distribution of $\bar{B} \to D\tau\bar{\nu}$ decay rate is helpful to discriminate two scalar operators.

It might be considered hard task to measure the tau longitudinal polarization due to the missing neutrinos in the final state. The τ in $\bar{B} \to D^{(*)}\tau\bar{\nu}$ is identified by $\tau \to \pi\nu$ or $\tau \to \ell\bar{\nu}\nu$ ($\ell = e, \mu$) in the present B factory experiments[4]. Here we show how these decay modes work as τ polarization analyzer. We use a coordinate system in the q rest frame such that the direction of the $\bar{B}$ and $D^{(*)}$ momenta is the z axis, and the τ momentum lies in the x-z plane. Then, we parameterize the τ momentum as $p^\mu_\tau = E_\tau(1, \beta_\tau \sin\theta_\tau, 0, \beta_\tau \cos\theta_\tau)$,

[3] It is possible to define two distinct and independent τ polarizations, namely the transverse polarization and the longitudinal one. While the transverse polarization is generated by T violating interactions and/or final state interactions, the longitudinal polarization is sensitive to the chiral structure of the relevant interactions which we want to study.

[4] The recent BABAR study [7] has used only the pure leptonic mode $\tau \to \ell\bar{\nu}\nu$. This choice leads to the cancellation of various sources of uncertainty in the ratios $R(D^{(*)})$, because the signal $\bar{B} \to D^{(*)}\tau\bar{\nu}$ and normalization $\bar{B} \to D^{(*)}\ell\bar{\nu}$ events are identified by the same particles in the final state.

where $E_\tau = (q^2 + m_\tau^2)/(2\sqrt{q^2})$ and $\beta_\tau = \sqrt{1 - m_\tau^2/E_\tau^2}$. The differential rate of the decay chain $\bar{B} \to M\tau\bar{\nu}$ ($M = D, D^*$) followed by $\tau \to X$ is written as

$$\frac{d\Gamma}{dq^2 d\zeta_X}(\bar{B} \to M(\tau \to X)\bar{\nu}) = \mathcal{B}(\tau \to X)\frac{d\Gamma(M)}{dq^2}\left[f_X(q^2, \zeta_X) + P_\tau(M; q^2)\, g_X(q^2, \zeta_X)\right], \quad (93)$$

where $\Gamma(M) = \Gamma(M)^+ + \Gamma(M)^-$ is the total decay rate of $\bar{B} \to M\tau\bar{\nu}$ as defined in Eq. (57), $P_\tau(M; q^2)$ is the q^2 distribution of $P_\tau(M)$, and ζ_X is represented as

$$\zeta_{\pi\nu} = \frac{E_\pi}{E_\tau}, \quad \zeta_{\ell\bar{\nu}\nu} = \frac{E_\ell}{E_\tau}, \quad (94)$$

where $E_{\pi(\ell)}$ is the $\pi(\ell)$ energy in the q rest frame and $\mathcal{B}(\tau \to X)$ denotes the branching fraction of $\tau \to X$. The functions f_X and g_X for $\tau \to \pi\nu$ are well-known and given by

$$f(q^2, \zeta) = 1/\beta_\tau\,, \quad g(q^2, \zeta) = (2\zeta - 1)/\beta_\tau^2\,, \quad (95)$$

where we neglect the pion mass and omit the subscript for simplicity. The range of ζ is $(1 - \beta_\tau)/2 \le \zeta \le (1 + \beta_\tau)/2$. As for $\tau \to \ell\bar{\nu}\nu$, ignoring the ℓ mass, the decay distribution is described by

$$f(q^2, \zeta) = \frac{16}{3}\frac{\zeta^2}{(1 - \beta_\tau^2)^3}[9(1 - \beta_\tau^2) - 4(3 + \beta_\tau^2)\zeta]\,, \quad (96)$$

$$g(q^2, \zeta) = -\frac{16}{3}\frac{\zeta^2}{(1 - \beta_\tau^2)^3}\beta_\tau[3(1 - \beta_\tau^2) - 16\zeta]\,, \quad (97)$$

for $0 \le \zeta \le (1 - \beta_\tau)/2$, and

$$f(q^2, \zeta) = \frac{1 + \beta_\tau - 2\zeta}{3\beta_\tau(1 + \beta_\tau)^3}[5(1 + \beta_\tau)^2 + 10(1 + \beta_\tau)\zeta - 16\zeta^2]\,, \quad (98)$$

$$g(q^2, \zeta) = \frac{1 + \beta_\tau - 2\zeta}{3\beta_\tau(1 + \beta_\tau)^3}\frac{1}{\beta_\tau}[(1 + \beta_\tau)^2 + 2(1 + \beta_\tau)\zeta - 8(1 + 3\beta_\tau)\zeta^2]\,, \quad (99)$$

for $(1 - \beta_\tau)/2 \le \zeta \le (1 + \beta_\tau)/2$. In is noted that the $P_\tau(M; q^2)$ term in Eq. (93) vanish when the function g_X is integrated over ζ_X. Accordingly we can determine $P_\tau(M; q^2)$ by measuring the ζ_X distribution for fixed q^2 in Eq. (93). As a result, the polarization as defined in Eq. (91) is obtained by integrating $P_\tau(M; q^2)$ over q^2.

The statistical uncertainty of the ideal experiment is given by [42, 43]

$$\delta P_\tau^X(M; q^2) = \frac{1}{\sqrt{N(q^2)}S_X(M; q^2)}\,, \quad (100)$$

where $N(q^2)$ is the number of signal events for fixed q^2 (or in a bin of q^2, more practically) and $S_X(M; q^2)$ indicates "sensitivity" for measuring the tau polarization by use of successive

tau decay $\tau \to X$ and is written as

$$S_X(M;q^2) = \left[\int d\zeta \frac{g_X^2(q^2,\zeta_X)}{f_X(q^2,\zeta_X) + P_\tau(M;q^2) g_X(q^2,\zeta_X)}\right]^{1/2}. \tag{101}$$

For the integrated polarization $P_\tau(M)$, we obtain

$$\delta P_\tau^X(M) = \frac{1}{\sqrt{N}\, S_X(M)}, \tag{102}$$

where N is the total number of signal events and the integrated sensitivity S is given by

$$S_X(M) = \left[\frac{1}{\Gamma(M)} \int dq^2 \frac{d\Gamma(M)}{dq^2} \frac{1}{S_X(M;q^2)^2}\right]^{-1/2}. \tag{103}$$

Assuming the SM and neglecting the uncertainties in the form factors, we obtain

$$S_{\pi\nu}(D) = 0.60, \quad S_{\ell\bar{\nu}\nu}(D) = 0.23, \tag{104}$$

$$S_{\pi\nu}(D^*) = 0.61, \quad S_{\ell\bar{\nu}\nu}(D^*) = 0.20. \tag{105}$$

These values vary less than 20% even in the presence of new physics taking the constraint from the branching fraction into account. Thus we can naively evaluate the expected uncertainties in the measurements of $P_\tau(D^{(*)})$. For example, the expected uncertainties in $P_\tau(D^{(*)})$ are calculated as

$$\frac{\delta P_\tau^{\ell\bar{\nu}\nu}(D)}{P_\tau(D)} = 0.60, \quad (N \sim 500) \tag{106}$$

$$\frac{\delta P_\tau^{\ell\bar{\nu}\nu}(D^*)}{P_\tau(D^*)} = 0.35, \quad (N \sim 900) \tag{107}$$

in the SM, where the number of the signal event is based on the recent BABAR study [7]. Then we find the present experiments do not have the ability to measure the polarizations with sufficient accuracies due to less statistics. At the super B factory with integrated luminosity of $50\,\mathrm{ab}^{-1}$, $N \sim 2000$ and $N \sim 5000$ for the decays $\bar{B} \to D\tau\bar{\nu}$ and $\bar{B} \to D^*\tau\bar{\nu}$ identified by $\tau \to \pi\nu$ are obtained based on the Monte Carlo simulation in Ref. [44]. Similarly, $N \sim 5000$ and $N \sim 8000$ for the decays identified by $\tau \to \ell\bar{\nu}\nu$ are obtained. Thus the corresponding expected uncertainties are estimated as

$$\frac{\delta P_\tau^{\ell\bar{\nu}\nu}(D)}{P_\tau(D)} = 0.24, \quad \frac{\delta P_\tau^{\pi\nu}(D)}{P_\tau(D)} = 0.11, \tag{108}$$

$$\frac{\delta P_\tau^{\ell\bar{\nu}\nu}(D^*)}{P_\tau(D^*)} = 0.11, \quad \frac{\delta P_\tau^{\pi\nu}(D^*)}{P_\tau(D^*)} = 0.05. \tag{109}$$

We can see that the polarizations with sufficient accuracies will be measured at the super B factory.

B. New physics effect

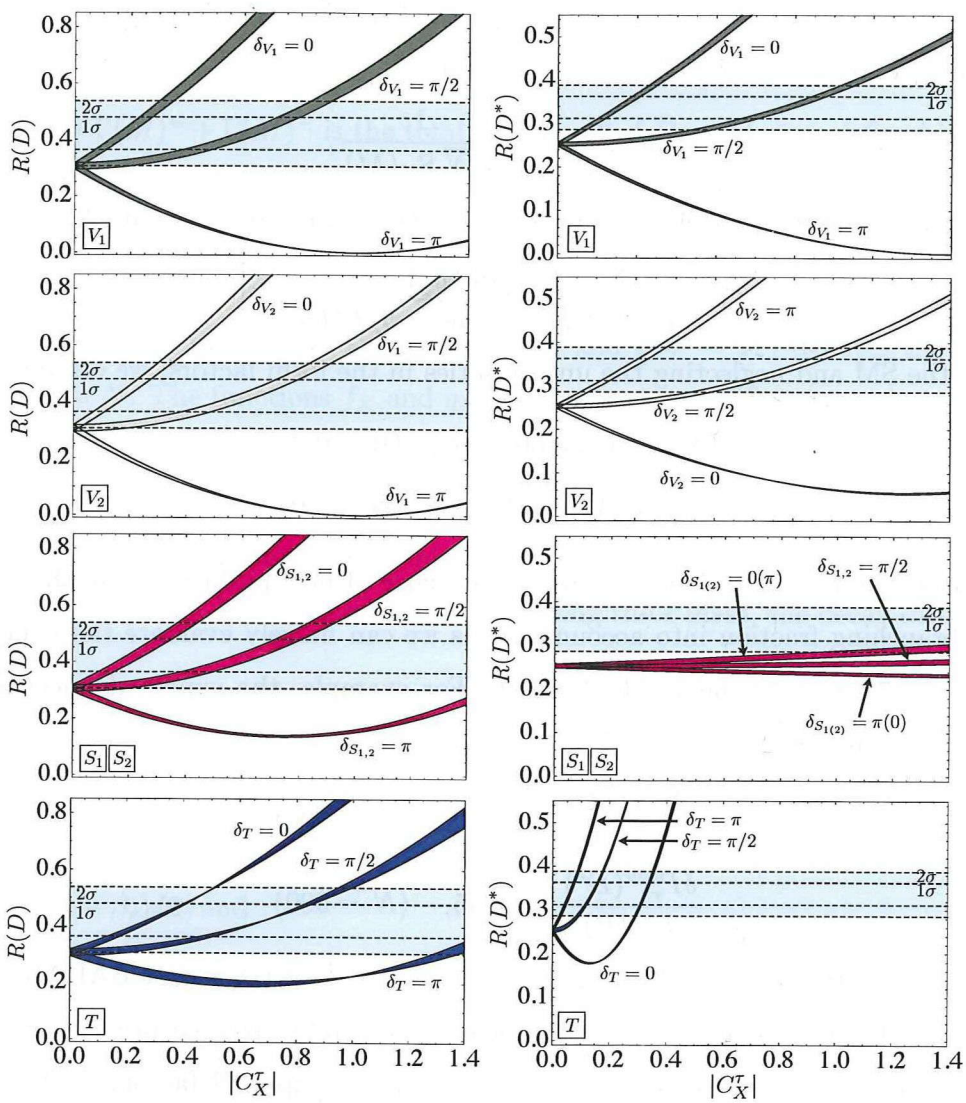

FIG. 4: Predictions on the branching ratios as functions of the absolute value of Wilson coefficient $|C_X^c|$ for $X = V_{1,2}, S_{1,2}, T$. The predictions of new physics effects for the operators $\mathcal{O}_X^{cv\ell}$ are given by the lines for $\delta_X = \pi/2$ in these graphs. The light blue horizontal bands represent the experimental values.

As shown above, it is worth studying the new physics effects on the polarizations while they have not been measured yet. In Figs. 4 and 5, we show new physics effects on $R(D^{(*)})$, $P_\tau(D^{(*)})$ and P_{D^*}. The horizontal axis is $|C_X^c|$ and three cases of $\delta_X = 0, \pi/2$, and π are shown for illustration, where δ_X is the complex phase of C_X^c. Effects of $\mathcal{O}_X^{cv\ell}$ are the same

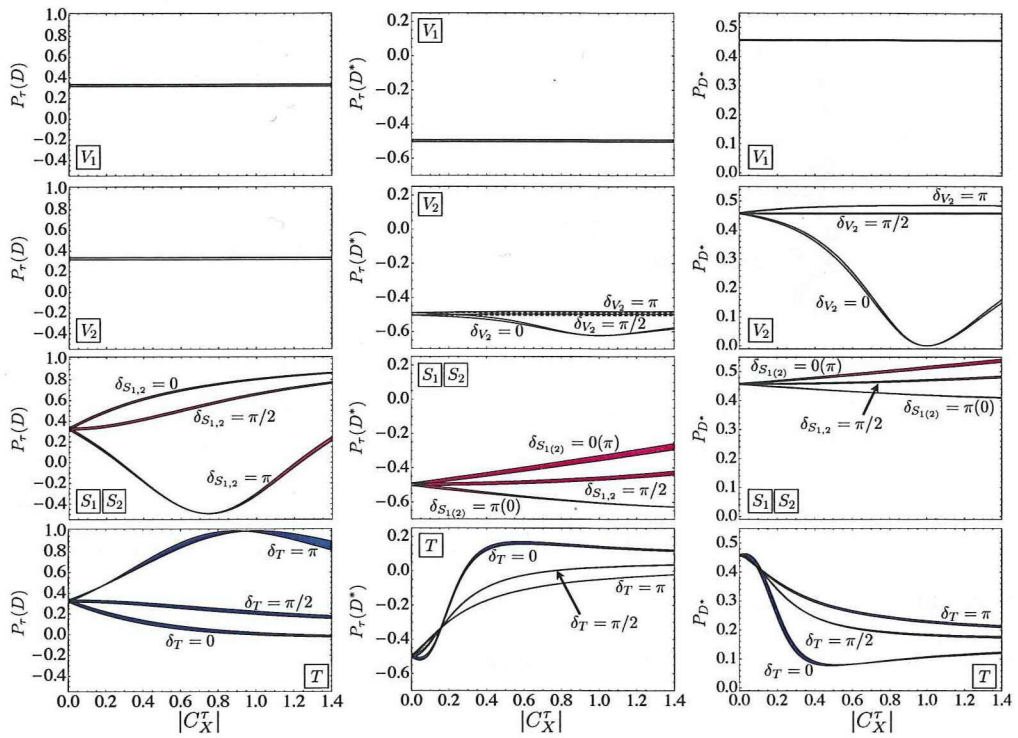

FIG. 5: Predictions on $P_\tau(D), P_\tau(D^*)$ and P_{D^*} as functions of $|C_X^c|$ for $X = V_{1,2}, S_{1,2}, T$. The predictions of new physics effects for the operators $\mathcal{O}_X^{c\nu_\ell}$ are given by the lines for $\delta_X = \pi/2$.

as those of $\mathcal{O}_X^c$ with $\delta_X = \pi/2$ as mentioned above. The width of each prediction indicates uncertainties due to the form factors. We include $\pm 100\%$ errors in the overall magnitudes of $\Delta(w)$ and $\Delta_3(w)$ as uncertainties in addition to the ranges of $\rho_1^2, \rho_{A_1}^2, R_1(1)$ and $R_2(1)$. The horizontal bands with dashed boundaries in Fig. 4 represent the experimental values given in Table II. From these results, we find that the sensitivity to the magnitude of the Wilson coefficient varies depending on each operator. We note that the theoretical uncertainties are sufficiently smaller than the present experimental accuracy. Therefore, we use the central values of the theoretical predictions in the rest of this work unless otherwise stated.

C. Different standpoint: correlation between $R(D)$ and $R(D^*)$

Since we have seen that each new physics operator contributes to observables in different ways as shown in Figs. 4 and 5, it is useful to examine correlations among observables for the sake of discrimination of new physics operators. Here we study the correlation between $R(D)$ and $R(D^*)$. In the left panel of Fig. 6, we show $R(D)$ and $R(D^*)$ in the presence of

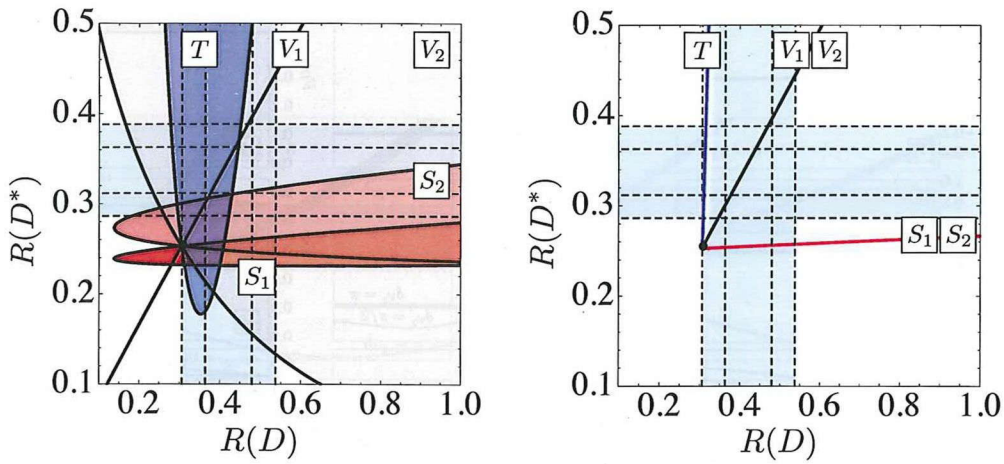

FIG. 6: Correlations between $R(D)$ and $R(D^*)$ in the presence of new physics operators of $\mathcal{O}_X^c$ (left) and $\mathcal{O}_X^{cv\ell}$ (right) for $X = V_{1,2}, S_{1,2}, T$. The black dot in each panel indicates the SM prediction. The light blue horizontal and vertical bands are the experimental values.

the new physics operators for $\mathcal{O}_X^c$ ($X = V_{1,2}, S_{1,2}$ and T). The shaded regions are predicted by the indicated operators. As is known [28], $R(D)$ is more sensitive to the scalar type operators $\mathcal{O}_{S_1}^c$ and $\mathcal{O}_{S_2}^c$ than $R(D^*)$. This is due to the angular momentum conservation that gives an extra suppression factor for the vector meson. On the other hand, we find that the tensor type operator $\mathcal{O}_T^c$ exhibits the opposite behavior, that is, $R(D^*)$ is more sensitive to $\mathcal{O}_T^c$ than $R(D)$. The vector type operator $\mathcal{O}_{V_1}^c$ gives a unique relation between $R(D)$ and $R(D^*)$, since it is just the SM operator and changes only the overall factor. The vector type operator $\mathcal{O}_{V_2}^c$ that contains the right-handed quark current covers a wide region in this plane.

The correlations between $R(D)$ and $R(D^*)$ for the neutrino flavor violating operators $\mathcal{O}_X^{cv\ell}$ are shown in the right panel of Fig. 6. As these operators do not interfere with the SM one, they always increase $R(D)$ and $R(D^*)$ with different ratios depending on X.

Once a future experiment gives precise values of $R(D)$ and $R(D^*)$, we may exclude some operators depending on the actual experimental values.

D. Different standpoint: correlations between decays rates and polarizations

As shown in Fig. 5, polarizations are also useful observables to identify new physics. Here we show correlations between decay rates and polarizations in Fig. 7. The gray horizontal

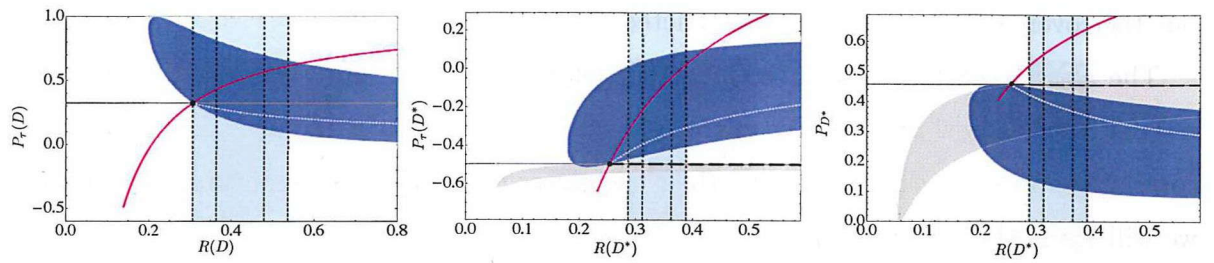

FIG. 7: Correlations between $R(D^{(*)})$ and $P_\tau(D^{(*)})$, and $R(D^*)$ and P_{D^*} in the presence of new physics operators $\mathcal{O}_{V_1}^{c,c\nu_\ell}$ (gray horizontal lines), $\mathcal{O}_{V_2}^{c}$ (light gray regions), $\mathcal{O}_{V_2}^{c\nu_\ell}$ (black dashed lines), $\mathcal{O}_{S_{1,2}}^{c,c\nu_\ell}$ (magenta curves), $\mathcal{O}_{T}^{c}$ (blue regions) and $\mathcal{O}_{T}^{c\nu_\ell}$ (white dotted curves). The black dot in each panel indicates the SM prediction. The light blue vertical bands show the experimental constraints.

lines represent the correlations for $\mathcal{O}_{V_1}^{c,c\nu_\ell}$, the light gray regions (black dashed lines) for $\mathcal{O}_{V_2}^{c(\nu_\ell)}$, the magenta curves for the scalar operators $\mathcal{O}_{S_{1,2}}^{c,c\nu_\ell}$, and the blue regions (white dotted curves) for $\mathcal{O}_{T}^{c(\nu_\ell)}$. The operator $\mathcal{O}_{V_2}^{c\nu_\ell}$ gives the same line as $\mathcal{O}_{V_1}^{c\nu_\ell}$ in $\bar{B} \to D\tau\bar{\nu}$. The light blue vertical bands show the experimental constraints on $R(D)$ and $R(D^*)$.

We find specific features of the scalar operators in this figure. The polarizations $P_\tau(D^{(*)})$ and P_{D^*} are uniquely related to the corresponding decay rates in the presence of scalar operators, because the scalar operators $\mathcal{O}_{S_1}^{c}$ and $\mathcal{O}_{S_2}^{c}$ contribute only to $\Gamma^+(D^{(*)})$ and $\Gamma(D_L^*)$. The definitions of polarizations may be rewritten as

$$\left[\Gamma^+(D^{(*)}) + \Gamma^-(D^{(*)})\right]\left[1 - P_\tau(D^{(*)})\right] = 2\Gamma^-(D^{(*)})\,, \tag{110}$$

$$\left[\Gamma(D_T^*) + \Gamma(D_L^*)\right](1 - P_{D^*}) = \Gamma(D_T^*)\,. \tag{111}$$

The right-hand sides of these equations are given solely by the SM contributions, and thus the polarizations are definitely determined by the corresponding decay rates as seen in Fig. 7. These specific correlations are prominent predictions of the scalar type operators, although we cannot discriminate $\mathcal{O}_{S_1}^{c}$ from $\mathcal{O}_{S_2}^{c}$ by using these correlations.

As for the other operators, it is apparent that the SM operator $\mathcal{O}_{V_1}^{c}$ and $\mathcal{O}_{V_1}^{c\nu_\ell}$ do not affect the polarizations. While the quark right handed current $\mathcal{O}_{V_2}^{c(\nu_\ell)}$ has no effect on the tau polarization in $\bar{B} \to D\tau\bar{\nu}$ because the axial vector part does not contribute to this process. The operator $\mathcal{O}_{V_2}^{c\nu_\ell}$ in $\bar{B} \to D^*\tau\bar{\nu}$ and the tensor operator $\mathcal{O}_{T}^{c\nu_\ell}$ in both the processes predict definite relations between the polarizations and the rates. The operator $\mathcal{O}_{V_2}^{c}$ in $\bar{B} \to D^*\tau\bar{\nu}$ and the tensor operator $\mathcal{O}_{T}^{c}$ in both the processes have no such specific relations,

but the covered regions are rather restricted.

The above correlations that include the polarizations definitely increase the ability to restrict possible new physics. We might uniquely identify the new physics operator by these correlations in some cases. However their usefulness depends on experimental situations as we will see in the next section.

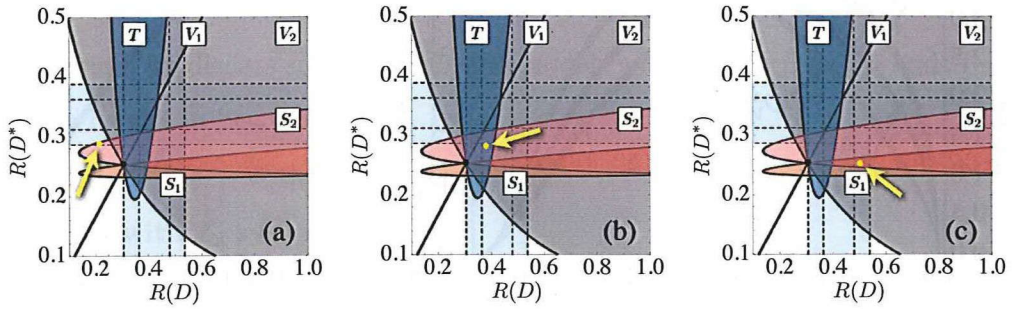

FIG. 8: Three examples for the discrimination of new physics contribution: (a) $R(D) = 0.21$, $R(D^*) = 0.29$, (b) $R(D) = 0.37$, $R(D^*) = 0.28$ and (c) $R(D) = 0.51$, $R(D^*) = 0.25$.

	(a)	(b)			(c)		
$(R(D), R(D^*))$	$(0.21, 0.29)$	$(0.37, 0.28)$			$(0.51, 0.25)$		
X	S_2	S_2	V_2	T	S_1	S_2	V_2
C_X^c	$-1.20 \pm i\,0.18$	$-0.81 \pm i\,0.87$	$0.03 \pm i\,0.40$	$0.16 \pm i\,0.14$	$-0.50 \pm i\,1.08$	$0.21 \pm i\,0.56$	$0.18 \pm i0.53$
$P_\tau(D)$	0.02	0.44	0.33	0.22	0.60	0.60	0.33
$P_\tau(D^*)$	-0.30	-0.35	-0.50	-0.26	-0.51	-0.51	-0.50
P_{D^*}	0.53	0.51	0.45	0.32	0.45	0.45	0.44

TABLE III: Predictions for the polarizations in each of three cases.

V. MODEL INDEPENDENT ANALYSIS

In this section, we illustrate several possibilities to restrict or identify new physics using the observables discussed in the previous section and decay distributions. We suppose that $R(D)$ and $R(D^*)$ will be measured more precisely in a future super B factory experiment. Then we will determine the Wilson coefficient C_X^c associated with $\mathcal{O}_X^c$ that is assumed to be dominant except for the SM contribution and predict other observables.

Here we consider the following three cases of $(R(D), R(D^*))$:

(a) $(0.21, 0.29)$ as shown in Fig. 8(a), in which $\mathcal{O}_{S_2}^c$ is unambiguously identified as the new physics operator.

(b) $(0.37, 0.28)$ as shown in Fig. 8(b), in which $\mathcal{O}_{S_2}^c, \mathcal{O}_{V_2}^c$, and $\mathcal{O}_T^c$ are the candidates for the new physics operator.

(c) $(0.51, 0.25)$ as shown in Fig. 8(c), in which $\mathcal{O}_{S_1}^c, \mathcal{O}_{S_2}^c$, and $\mathcal{O}_{V_2}^c$ are possible.

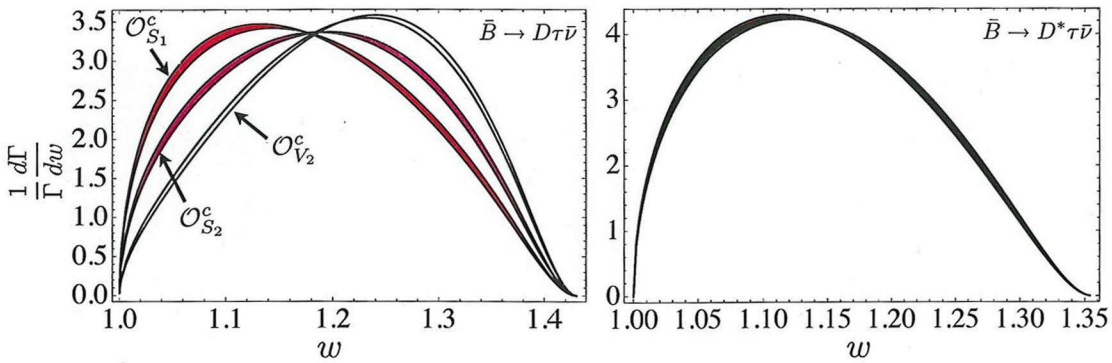

FIG. 9: Distributions of w in $\bar{B} \to D\tau\bar{\nu}$ and $\bar{B} \to D^*\tau\bar{\nu}$ for the case (c), wehre $w = (m_B^2 - m_M^2 - q^2)/(2m_B m_M)$. The red, magenta, and light gray regions represent the distributions in the cases of $\mathcal{O}^c_{S_1}, \mathcal{O}^c_{S_2}$ and $\mathcal{O}^c_{V_2}$ respectively, including the theoretical uncertainties. The w distributions in $\bar{B} \to D^*\tau\bar{\nu}$ are almost identical for the three operators.

One of $R(D)$ and $R(D^*)$ is chosen to be within the 2σ range but the other is allowed to deviate more. We note that $\mathcal{O}_X^{c\nu_\ell}$ do not reproduce the assumed sets of $R(D)$ and $R(D^*)$. Table III summarizes the Wilson coefficient and the predicted polarizations for each case.

In the case (a), the dominant new physics operator is uniquely determined to be $\mathcal{O}^c_{S_2}$. The polarizations can be used to confirm that the deviation from the SM comes from the operator $\mathcal{O}^c_{S_2}$. Furthermore the assumption of one-operator dominance will be tested.

In the case (b), the dominant operator is $\mathcal{O}^c_{S_2}, \mathcal{O}^c_{V_2}$, or $\mathcal{O}^c_T$. The predicted values of polarizations vary from operator to operator. We will determine the dominant new physics operator by measuring $P_\tau(D^*)$ for example. Then the one-operator dominance will be checked by looking up other polarizations.

In the case (c), the dominant operator is $\mathcal{O}^c_{S_1}, \mathcal{O}^c_{S_2}$, or $\mathcal{O}^c_{V_2}$. The occurrence of $\mathcal{O}^c_{V_2}$ is distinguished from that of $\mathcal{O}^c_{S_1}$ or $\mathcal{O}^c_{S_2}$ by polarizations. Two scalar operators $\mathcal{O}^c_{S_1}$ and $\mathcal{O}^c_{S_2}$, however, predict the same values of the polarizations as explained in Sec. IV D. Under such a situation, q^2 distributions may discriminate between $\mathcal{O}^c_{S_1}$ and $\mathcal{O}^c_{S_2}$. In Fig. 9, we present q^2 distributions for $\mathcal{O}^c_{S_1}$, $\mathcal{O}^c_{S_2}$, and $\mathcal{O}^c_{V_2}$ in the case (c). We note that the abscissa is $w = (m_B^2 - m_M^2 - q^2)/(2m_B m_M)$ instead of q^2. The q^2 distribution in $\bar{B} \to D\tau\bar{\nu}$ turns out to be useful for the discrimination in this case.

VI. MODEL ANALYSIS

In this section, we discuss some new physics models which affect $\bar{B} \to \tau\bar{\nu}$ and $\bar{B} \to D^{(*)}\tau\bar{\nu}$ based on the results in Sec. III.

A. 2HDM with Z_2 symmetry

As known well, the charged Higgs boson in two Higgs doublet models (2HDMs) contributes to the tauonic B meson decays and its effect is enhanced in some cases. In order to forbid flavor changing neutral currents (FCNC) at the tree level, a Z_2 symmetry is often imposed in this class of models and it results in four distinct 2HDMs [45–48] . Their Yukawa terms are described as

$$\mathcal{L}_{\rm Y} = -\bar{Q}_L Y_u \tilde{H}_2 u_R - \bar{Q}_L Y_d H_2 d_R - \bar{L}_L Y_\ell H_2 \ell_R + \text{h.c.} \quad \text{(type I)}, \tag{112}$$

$$\mathcal{L}_{\rm Y} = -\bar{Q}_L Y_u \tilde{H}_2 u_R - \bar{Q}_L Y_d H_1 d_R - \bar{L}_L Y_\ell H_1 \ell_R + \text{h.c.} \quad \text{(type II)}, \tag{113}$$

$$\mathcal{L}_{\rm Y} = -\bar{Q}_L Y_u \tilde{H}_2 u_R - \bar{Q}_L Y_d H_2 d_R - \bar{L}_L Y_\ell H_1 \ell_R + \text{h.c.} \quad \text{(type X)}, \tag{114}$$

$$\mathcal{L}_{\rm Y} = -\bar{Q}_L Y_u \tilde{H}_2 u_R - \bar{Q}_L Y_d H_1 d_R - \bar{L}_L Y_\ell H_2 \ell_R + \text{h.c.} \quad \text{(type Y)}, \tag{115}$$

where $H_{1,2}$ are Higgs doublets defined as

$$H_i = \begin{pmatrix} h_i^+ \\ (v_i + h_i^0)/\sqrt{2} \end{pmatrix}, \quad \tilde{H}_i = i\sigma_2 H_i, \tag{116}$$

and v_i denotes the vacuum expectation value (VEV) of H_i. The ratio of two VEVs is defined as $\tan\beta = v_2/v_1$ and $v = \sqrt{v_1^2 + v_2^2} = 246\text{GeV}$. In type I, all masses of quarks and leptons are given by the VEV of H_2. In type II, the up-type quarks obtain their masses from H_2, while the down-type quarks and leptons from H_1. In type X, H_2 and H_1 are responsible to the quark and lepton masses respectively. The masses of the down-type quarks are given by H_1 and other fermions acquire their masses from H_2 in type Y. Under this definition v_2 generates up-quark masses in any types of Yukawa interaction.

These 2HDMs contain a pair of physical charged Higgs bosons, which contributes to $\bar{B} \to \tau\bar{\nu}$ and $\bar{B} \to D^{(*)}\tau\bar{\nu}$ as shown in Fig. 10. The relevant Wilson coefficients introduced

	Type I	Type II	Type X	Type Y
ξ_d	$\cot^2\beta$	$\tan^2\beta$	-1	-1
ξ_u	$-\cot^2\beta$	1	1	$-\cot^2\beta$

TABLE IV: Parameters $\xi_{d,u}$ in each type of 2HDMs.

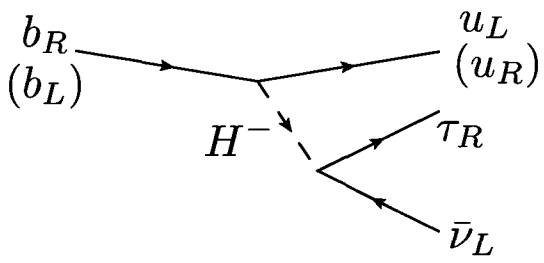

FIG. 10: Charged Higgs contribution to the decays.

in Eq. (2) are represented as

$$C_{S_1}^u = C_{S_1}^c = -\frac{m_b m_\tau}{m_{H^\pm}^2}\xi_d\,, \tag{117}$$

$$C_{S_2}^u = -\frac{m_u m_\tau}{m_{H^\pm}^2}\xi_u, \quad C_{S_2}^c = -\frac{m_c m_\tau}{m_{H^\pm}^2}\xi_u\,, \tag{118}$$

where $m_{H^\pm}$ is the mass of the charged Higgs boson. The parameters ξ_d and ξ_u are presented in Table IV. One can see that the charged Higgs interaction which corresponds to $\mathcal{O}_{S_1}^{u,c}$ affect $\bar{B} \to \tau\bar{\nu}$ and $\bar{B} \to D^{(*)}\tau\bar{\nu}$ in the same fashion. For the operator $\mathcal{O}_{S_2}^q$, the contribution of the charged Higgs to $\bar{B} \to \tau\bar{\nu}$ is very suppressed due to the small up quark mass. As explained in Sec. I, a sizable new physics effect is needed in order to explain the experimental measurement on $R(D^{(*)})$, while the SM prediction on the branching ratio in $\bar{B} \to \tau\bar{\nu}$ is sufficiently consistent with the experimental result. Thus it is naively expected that $\mathcal{O}_{S_2}^q$ in the 2HDMs is suitable to explain the recent experimental results in $\bar{B} \to \tau\bar{\nu}$ and $\bar{B} \to D^{(*)}\tau\bar{\nu}$ at the same time. To have a sizable charged Higgs effect, $|\xi_{d,u}|$ should be much larger than unity taking the experimental bound on the charged Higgs mass into account. Then the case of $\xi_u = 1$ or $\xi_d = -1$ is not acceptable. The case of $\xi_u = -\cot^2\beta$ or $\xi_d = \cot^2\beta$ with $\cot^2\beta \gg 1$ is unnatural since the top Yukawa interaction becomes nonperturbative. The requirement for the top Yukawa interaction to be perturbative results in $\tan\beta \gtrsim 0.4$ [48]. Therefore, the operator $\mathcal{O}_{S_2}^c$ cannot have sizable effect on $\bar{B} \to D^{(*)}\tau\bar{\nu}$ in the 2HDM. While

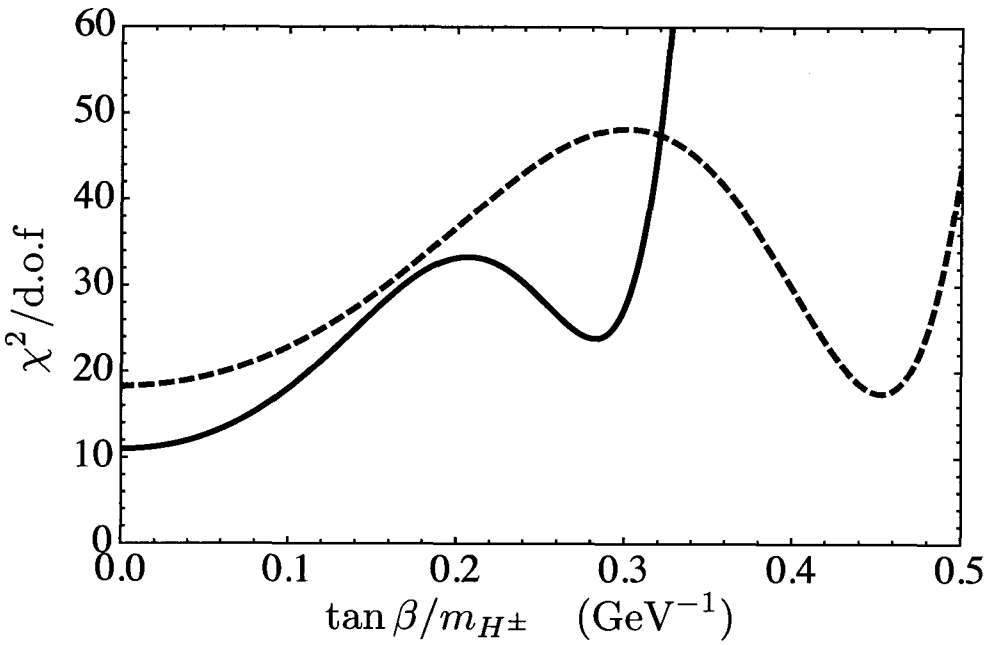

FIG. 11: Fit to $\tan\beta/m_{H^\pm}$ using both $\bar{B} \to \tau\bar{\nu}$ and $\bar{B} \to D^{(*)}\tau\bar{\nu}$ (black line), and only $\bar{B} \to D^{(*)}\tau\bar{\nu}$ (black dashed line).

the type II of $\xi_d = \tan^2\beta$ is only the case to be sizable and only $C_{S_1}^{u,c}$ in the 2HDM of type II is potentially enhanced. As we have shown in Sec. III, however, it is difficult to explain the current experimental results in $\bar{B} \to D^{(*)}\tau\bar{\nu}$ by $\mathcal{O}_{S_1}^c$ alone.

The analysis that depend on a model has the benefit of relating another quantities. In the 2HDM, the contributions of the charged Higgs boson to $\bar{B} \to \tau\bar{\nu}$ and $\bar{B} \to D^{(*)}\tau\bar{\nu}$ are represented as the same variable as in Eq. (117). In Fig. 11, we show χ^2 analysis of the charged Higgs parameter $\tan\beta/m_{H^\pm}$ in the 2HDM of type II. The Black line indicates the result of combined analysis using the experimental data of $\bar{B} \to \tau\bar{\nu}$ and $\bar{B} \to D^{(*)}\tau\bar{\nu}$. The Black dashed line represents the result using only $\bar{B} \to D^{(*)}\tau\bar{\nu}$. Then we find that the operator $\mathcal{O}_{S_1}^{u,c}$ in the 2HDM of type II for the largely contributed region is disfavored with more than 99.9% CL. It is noted that for the region near the SM prediction, the confidence level of exclusion from $\bar{B} \to \tau\bar{\nu}$ and $\bar{B} \to D^{(*)}\tau\bar{\nu}$ is smaller than that from only $\bar{B} \to D^{(*)}\tau\bar{\nu}$. This is because the result of $\bar{B} \to \tau\bar{\nu}$ is near consistent with the SM prediction. The exclusion for the sizable effect of $\tan\beta/m_{H^\pm}$ is more powerful than the study in Ref. [7].

B. 2HDM allowing tree level FCNC

A possible solution within 2HDMs is to violate the Z_2 symmetry at the cost of FCNC. We introduce the following Z_2 breaking terms in the above four models:

$$\Delta\mathcal{L}_{\rm Y} = -\bar{Q}_L\epsilon''_u\tilde{H}_1 u_R - \bar{Q}_L\epsilon''_d H_1 d_R + \text{h.c.} \quad \text{(for type I and X)}, \tag{119}$$

$$\Delta\mathcal{L}_{\rm Y} = -\bar{Q}_L\epsilon''_u\tilde{H}_1 u_R - \bar{Q}_L\epsilon''_d H_2 d_R + \text{h.c.} \quad \text{(for type II and Y)}, \tag{120}$$

where $\epsilon''_{u,d}$ are 3×3 matrices that control FCNC and the quark fields are those in the weak basis. To obtain the charged Higgs interaction in the mass basis, first let us rotate the quark fields into

$$u_{L(R)} \to U_u^{L(R)} u_{L(R)}, \quad d_{L(R)} \to U_d^{L(R)} d_{L(R)}, \tag{121}$$

so as to diagonalize $Y_{u,d}$. Then, the mass matrices are rewritten as

$$M_u = \frac{1}{\sqrt{2}}\Big(v_2\, Y_u^D + v_1\, U_u^{L\dagger}\epsilon''_u U_u^R\Big), \tag{122}$$

$$M_d(x,y) = \frac{1}{\sqrt{2}}\left(x\, Y_d^D + y\, U_d^{L\dagger}\epsilon''_d U_d^R\right), \tag{123}$$

where $Y_{u,d}^D$ is the diagonal Yukawa matrix. The down-type quark mass term is represented as $M_d(v_2, v_1)$ for type I and X, and $M_d(v_1, v_2)$ for type II and Y. At this stage, the Yukawa terms are rewritten as

$$\mathcal{L}_{\rm Y} + \Delta\mathcal{L}_{\rm Y} = -\bar{u}_L V_{\rm CKM}^0 \left(\frac{Y_d^D}{\sqrt{2}}h_2^0 + \epsilon'_u h_1^+\right) d_R + \bar{d}_L V_{\rm CKM}^{0\dagger}\left(\frac{Y_u^D}{\sqrt{2}}h_2^0 + \epsilon'_u h_1^-\right) u_R + \text{h.c. (I,X)}, \tag{124}$$

$$\mathcal{L}_{\rm Y} + \Delta\mathcal{L}_{\rm Y} = -\bar{u}_L V_{\rm CKM}^0 \left(\frac{Y_d^D}{\sqrt{2}}h_2^0 + \epsilon'_u h_1^+\right) d_R + \bar{d}_L V_{\rm CKM}^{0\dagger}\left(\frac{Y_u^D}{\sqrt{2}}h_1^0 + \epsilon'_u h_2^-\right) u_R + \text{h.c. (II,Y)}, \tag{125}$$

where $V_{\rm CKM}^0 = U_u^{L\dagger}U_d^L$ is the Cabibbo-Kobayashi-Maskawa (CKM) matrix in the basis that diagonalize $Y_{u,d}$ and we define $\epsilon'_q = U_q^{L\dagger}\epsilon''_q U_q^R$ (for $q = u, d$). In turn, rotating the quark fields into

$$u_{L(R)} \to W_u^{L(R)} u_{L(R)}, \quad d_{L(R)} \to W_d^{L(R)} d_{L(R)}, \tag{126}$$

the mass matrices are diagonalized:

$$M_u^D = \frac{1}{\sqrt{2}}\Big(v_2\, W_u^{L\dagger} Y_u^D W_u^R + v_1\,\epsilon_u\Big), \tag{127}$$

$$M_d^D(x,y) = \frac{1}{\sqrt{2}}\Big(x\, W_d^{L\dagger} Y_d^D W_d^R + y\,\epsilon_d\Big), \tag{128}$$

	Z_u	Z_d	Z_ℓ
Type I	$\frac{\sqrt{2}M_u}{v}\cot\beta - \epsilon_u \sin\beta(1+\cot^2\beta)$	$-\frac{\sqrt{2}M_d}{v}\cot\beta + \epsilon_d \sin\beta(1+\cot^2\beta)$	$-\frac{\sqrt{2}M_\ell}{v}\cot\beta$
Type II	$\frac{\sqrt{2}M_u}{v}\cot\beta - \epsilon_u \cos\beta(\tan\beta+\cot\beta)$	$\frac{\sqrt{2}M_d}{v}\tan\beta - \epsilon_d \sin\beta(\tan\beta+\cot\beta)$	$\frac{\sqrt{2}M_\ell}{v}\tan\beta$
Type X	$\frac{\sqrt{2}M_u}{v}\cot\beta - \epsilon_u \sin\beta(1+\cot^2\beta)$	$-\frac{\sqrt{2}M_d}{v}\cot\beta + \epsilon_d \sin\beta(1+\cot^2\beta)$	$\frac{\sqrt{2}M_\ell}{v}\tan\beta$
Type Y	$\frac{\sqrt{2}M_u}{v}\cot\beta - \epsilon_u \cos\beta(\tan\beta+\cot\beta)$	$\frac{\sqrt{2}M_d}{v}\tan\beta - \epsilon_d \sin\beta(\tan\beta+\cot\beta)$	$-\frac{\sqrt{2}M_\ell}{v}\cot\beta$

TABLE V: The matrices $Z_{u,d,\ell}$ in each type of the 2HDM in the presence of the Z_2 breaking terms.

where we define $\epsilon_q = U_q^{W\dagger}\epsilon_q' W_q^R$. Then, rewriting the diagonal Yukawa coupling $Y_{u,d}^D$ in Eqs. (124) and (125) by use of the diagonalized quark masses $M_{u,d}^D$ and the extra coupling $\epsilon_{u,d}$ that induce FCNC, the physical charged Higgs and fermion interacting terms take the following form:

$$\mathcal{L}_{H^\pm} = \left(\bar{u}_R Z_u^\dagger V_{\rm CKM} d_L + \bar{u}_L V_{\rm CKM} Z_d d_R + \bar{\nu}_L Z_\ell \ell_R\right) H^+ + \text{h.c.}\,, \tag{129}$$

where $V_{\rm CKM} = W_u^{L\dagger} V_{\rm CKM}^0 W_d^L$ is the CKM matrix in the (true) quark mass basis. Table V shows the expressions of $Z_{u,d,\ell}$, where $M_{u,d,\ell}$ denote the diagonal up-type quark, down-type quark, and lepton mass matrices, and $\epsilon_{u,d}$ represent matrices $\epsilon_{u,d}''$ in the quark mass basis as defined above.

The FCNC in the down-quark sector is strongly constrained, so that ϵ_d^{ij} is negligible except for ϵ_d^{bb} in the present analysis. The relevant Wilson coefficients, which include ϵ_d^{bb} and the enhancement factor $\tan\beta$, are given by

$$C_{S_1}^u = C_{S_1}^c \simeq \frac{v m_\tau}{\sqrt{2} m_{H^\pm}^2} \epsilon_d^{bb} \sin\beta \tan^2\beta, \quad \text{(type II)}, \tag{130}$$

$$C_{S_1}^u = C_{S_1}^c \simeq -\frac{v m_\tau}{\sqrt{2} m_{H^\pm}^2} \epsilon_d^{bb} \sin\beta \tan\beta, \quad \text{(type X)}. \tag{131}$$

Although the positive interference to the SM contribution is possible depending on the sign of ϵ_d^{bb} even in the 2HDM of type II, the situation is almost the same as Eq. (117). In Fig. 12, we show the analysis for the fit to ϵ_d^{bb} in the 2HDM of type II assuming $\tan\beta = 50$ and $m_{H^\pm} = 500$GeV as a illustration. Even for allowing the positive interference to the SM contribution, the operator $\mathcal{O}_{S_1}^q$ in this model cannot explain the both results of pure and semi tauonic B decays.

On the other hand, constraints on the FCNC in the up quark sector are rather weak. Recently the 2HDM of type II that allows FCNC in the up quark sector is studied to explain

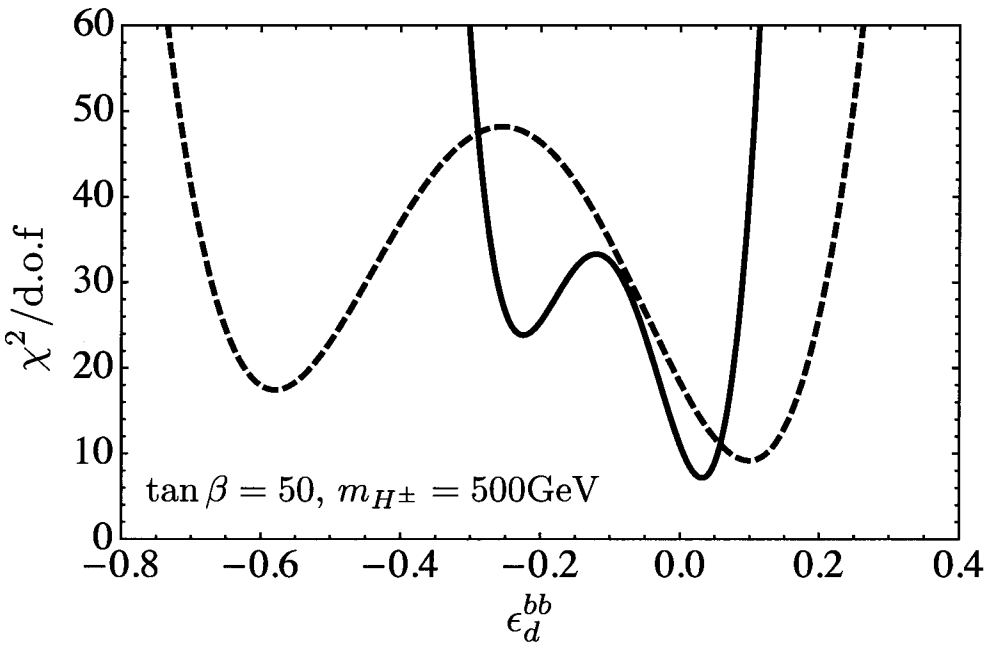

FIG. 12: Fit to ϵ_d^{bb} using both $\bar{B} \to \tau\bar{\nu}$ and $\bar{B} \to D^{(*)}\tau\bar{\nu}$ (black line), and only $\bar{B} \to D^{(*)}\tau\bar{\nu}$ (black dashed line). We assume that ϵ_d^{bb} is real, $\tan\beta = 50$ and $m_{H^\pm} = 500\text{GeV}$ as a illustration.

$\bar{B} \to \tau\bar{\nu}$ and $\bar{B} \to D^{(*)}\tau\bar{\nu}$ at the same time [41]. Table V implies that the operator $\mathcal{O}^c_{S_2}$ in types II and X might be significant for large $\tan\beta$. Then the corresponding Wilson coefficient is given by

$$C^c_{S_2} \simeq \frac{V_{tb}}{\sqrt{2}V_{cb}} \frac{vm_\tau}{m^2_{H^\pm}} (\epsilon_u^{tc})^* \sin\beta \tan\beta, \tag{132}$$

$$C^u_{S_2} \simeq \frac{V_{tb}}{\sqrt{2}V_{ub}} \frac{vm_\tau}{m^2_{H^\pm}} (\epsilon_u^{tu})^* \sin\beta \tan\beta. \tag{133}$$

In this case, the different components ϵ_u^{tu} and ϵ_u^{tc} of FCNC matrix are involved in $\bar{B} \to \tau\bar{\nu}$ and $\bar{B} \to D^{(*)}\tau\bar{\nu}$. As seen in Fig. 3 the current experimental results of $\bar{B} \to D^{(*)}\tau\bar{\nu}$ are described by the 2HDM of the type II or X with FCNC provided that $|\epsilon_u^{tc}| \sim 1$, while ϵ_u^{tu} is highly suppressed because of the enhancement factor V_{tb}/V_{ub}. If this is the case, we expect sizable deviations in polarizations $P_\tau(D^{(*)})$ and P_{D^*} from the SM as designated by the magenta curves in Fig. 7.

The large component ϵ_u^{tc} affects the top quark decay to charm quark. The Lagrangian which induces the FCNC process in the up-quark sector is given by

$$\mathcal{L}_{h,H} = \bar{u}_L \left[\frac{\cos(\alpha-\beta)}{\sqrt{2}\sin\beta} h + \frac{\sin(\alpha-\beta)}{\sqrt{2}\sin\beta} H + \frac{i}{\sqrt{2}\sin\beta} A \right] \epsilon_u u_R + \text{h.c.}, \tag{134}$$

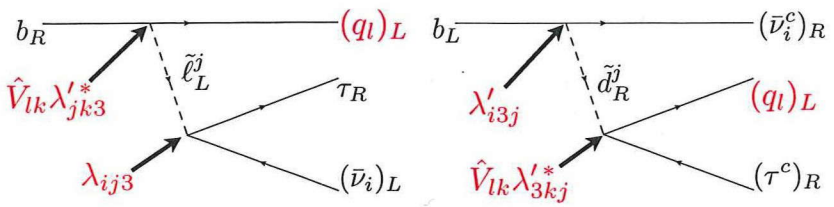

FIG. 13: Slepton and down squark contributions to the decays.

for all types of 2HDM, where $h(H)$ is the light(heavy) physical CP even Higgs, A is the CP odd Higgs, and α is a mixing angle between these two physical CP even Higgs. For example, let us consider the decay $t \to ch$. The decay rate $\Gamma(t \to ch)$ is calculated as

$$\Gamma(t \to ch) = \frac{|\epsilon_u^{tc}|^2}{64\pi} \frac{\cos^2(\alpha-\beta)}{\sin^2\beta} m_t \left(1 - \frac{m_h^2}{m_t^2}\right)^2 , \tag{135}$$

where $m_h \simeq 126\text{GeV}$ is obtained by the ATLAS [49] and CMS [50] experiments. While the dominant top quark decay is expected to be $t \to bW$. The decay rate $\Gamma(t \to bW)$ is represented as

$$\Gamma(t \to bW) = \frac{|V_{tb}|^2}{16\pi} \frac{m_t^3}{v^2} \left(1 - \frac{m_W^2}{m_t^2}\right)^2 \left(1 + 2\frac{m_W^2}{m_t^2}\right) . \tag{136}$$

Then the ratio of these decays is naively evaluated as

$$\frac{\Gamma(t \to ch)}{\Gamma(t \to bW)} \simeq 0.12 \frac{|\epsilon_u^{tc}|^2 \cos^2(\alpha-\beta)}{\sin^2\beta} . \tag{137}$$

Therefore, the large value $|\epsilon_u^{tc}| \sim 1$ desired for $\bar{B} \to D^{(*)}\tau\bar{\nu}$ gives at most 12% of the branching ratio of the top quark dominant decay $t \to bW$. The top quark decay to charm quark might be difficult to measure at the LHC experiment due to charm identification and good target for the ILC experiment.

The charged Higgs effects on $\bar{B} \to D^{(*)}\tau\bar{\nu}$ in the minimal supersymmetric standard model (MSSM) are the same as those in the 2HDM of type II at the tree level. Loop corrections induce non-holomorphic terms $\epsilon_{u,d}$ in Eq. (120) [51, 52]. However it seems difficult to enhance ϵ_u^{tc} to be $O(1)$. Thus the sufficient enhancement of $\mathcal{O}^c_{S_2}$ is unlikely in MSSM.

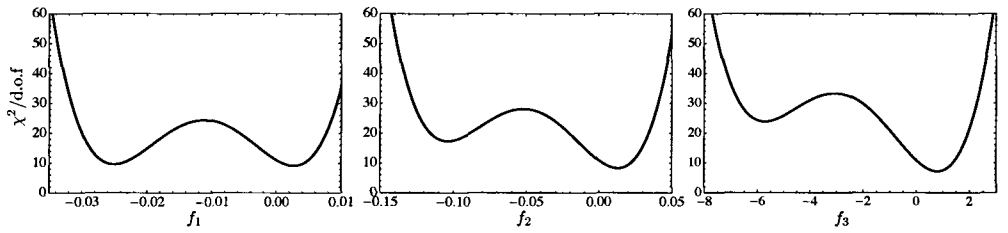

FIG. 14: Fit to f_k using both the experimental results of $\bar{B} \to \tau\bar{\nu}$ and $\bar{B} \to D^{(*)}\tau\bar{\nu}$. We assume that f_k is real and $m_{\tilde{l}^j_L} = 500\text{GeV}$ as an illustration.

C. MSSM with R-parity violation

The R-parity violating (RPV) MSSM [53] may also affect both $\bar{B} \to \tau\bar{\nu}$ [54, 55] and $\bar{B} \to D^{(*)}\tau\bar{\nu}$ [55–57]. We consider the following superpotential:

$$W_{\text{RPV}} = \frac{1}{2}\lambda_{ijk}L_iL_jE^c_k + \lambda'_{ijk}L_iQ_jD^c_k\,, \tag{138}$$

where λ_{ijk} and λ'_{ijk} are RPV couplings and i,j,k are generation indices. In general, the term $\lambda''U^cD^cD^c$, which is relevant to the proton decay, is involved in the R-parity violating theory, but it does not contribute to the decays we consider here at a tree level. Apart from the charged Higgs contribution, there are two kinds of diagrams which contribute to the tauonic B decays, that is, the slepton and down squark exchanging diagrams as shown in Fig. 13. The corresponding effective Lagrangian is written as

$$\mathcal{L}^{\text{RPV}}_{\text{eff}} = -\sum_{j,k=1}^{3}\hat{V}_{lk}\left[\frac{\lambda_{ij3}\lambda'^*_{jk3}}{m^2_{\tilde{l}^j_L}}(\bar{u}_l)_L b_R\,\bar{\tau}_R(\nu_i)_L + \frac{\lambda'_{i3j}\lambda'^*_{3kj}}{m^2_{\tilde{d}^j_R}}(\bar{u}_l)_L\,(\tau^c)_R\,(\bar{\nu}^c_i)_R\,b_L\right], \tag{139}$$

where $m_{\tilde{l}^j_L}$ ($m_{\tilde{d}^j_R}$) is the mass of the slepton (down squark) for the j-th generation and $\hat{V}_{ij} = V_{u_id_j}$ is a simple notation of the component of CKM matrix. Here we assume that the slepton and down squark mass matrices are diagonal in the super-CKM basis for simplicity. Using Fierz identity the second term in Eq. (139) is rewritten as

$$(\bar{u}_l)_L\,(\tau^c)_R\,(\bar{\nu}^c_i)_R\,b_L = \frac{1}{2}(\bar{u}_l)_L\gamma^\mu b_L\,\bar{\tau}_L\gamma_\mu(\nu_i)_L. \tag{140}$$

The RPV Lagrangian involves the interaction which induces the lepton flavor violation. In this case, $b \to q\tau\bar{\nu}$ with neutrino flavor being different from tau-lepton is included.

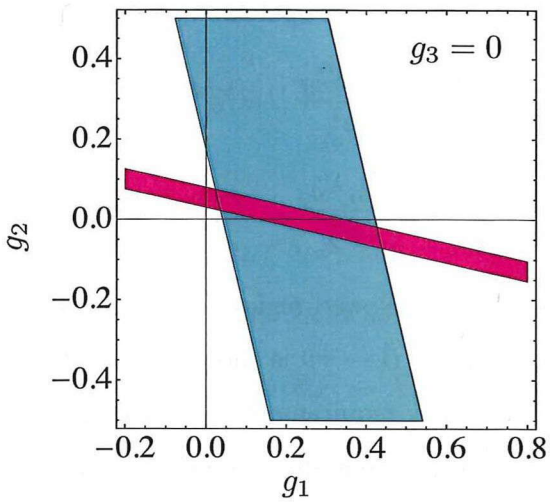

FIG. 15: An example of constraints on g_1 and g_2 assuming $g_3 = 0$. The magenta (cyan) region is allowed by the experimental results of $R(D^{(*)})$ ($\mathcal{B}(\bar{B} \to \tau\bar{\nu})$).

Then, the corresponding coefficients for the scalar type operators are expressed as

$$C^c_{S_1} = \frac{1}{2\sqrt{2}G_F V_{cb}} \sum_{j,k=1}^{3} \hat{V}_{2k} \frac{\lambda_{3j3}\lambda'^*_{jk3}}{m^2_{\tilde{\ell}^j_L}}, \quad C^{c\nu_\ell}_{S_1} = \frac{1}{2\sqrt{2}G_F V_{cb}} \sum_{j,k=1}^{3} \hat{V}_{2k} \frac{\lambda_{\ell j3}\lambda'^*_{jk3}}{m^2_{\tilde{\ell}^j_L}}, \tag{141}$$

$$C^u_{S_1} = \frac{1}{2\sqrt{2}G_F V_{ub}} \sum_{j,k=1}^{3} \hat{V}_{1k} \frac{\lambda_{3j3}\lambda'^*_{jk3}}{m^2_{\tilde{\ell}^j_L}}, \quad C^{u\nu_\ell}_{S_1} = \frac{1}{2\sqrt{2}G_F V_{cb}} \sum_{j,k=1}^{3} \hat{V}_{1k} \frac{\lambda_{\ell j3}\lambda'^*_{jk3}}{m^2_{\tilde{\ell}^j_L}}, \tag{142}$$

and we immediately see that the case that $C^{c(\nu_\ell)}_{S_1}$ is dominant contribution is disfavored as discussed in Sec. III. The combined fits to the product of the RPV couplings, which we define

$$f_k = \sum_{j=1}^{3} \lambda_{3j3}\lambda'^*_{jk3}, \tag{143}$$

are shown in Fig. 14. Here we assume that one of the f's for $k = 1, 2, 3$ contributes to $\bar{B} \to \tau\bar{\nu}$ and $\bar{B} \to D^{(*)}\tau\bar{\nu}$. We also assume all the slepton masses to be $m_{\tilde{\ell}^j_L} = 500\text{GeV}$ and f_k to be real as an illustration. Under this assumption, the contributions of f_k to the decays vary depending on $\hat{V}_{1k}$ and $\hat{V}_{2k}$ in $C^{u,c}_{S_1}$. We note that the result of the fit to f_3 is completely same as in Fig. 12 due to $C^c_{S_1} = C^u_{S_1}$ in this case. As a result, however, a sizable effect of any f_k turns out to be disfavored at more than 99% CL.

On the other hand, for the vector type operators, we obtain

$$C_{V_1}^{c} = \frac{1}{2\sqrt{2}G_F V_{cb}} \sum_{j,k=1}^{3} \hat{V}_{2k} \frac{\lambda'_{33j}\lambda'^{*}_{3kj}}{2m^2_{\tilde{d}^j_R}}, \quad C_{V_1}^{c\nu_\ell} = \frac{1}{2\sqrt{2}G_F V_{cb}} \sum_{j,k=1}^{3} \hat{V}_{2k} \frac{\lambda'_{\ell 3j}\lambda'^{*}_{3kj}}{2m^2_{\tilde{d}^j_R}}, \quad (144)$$

$$C_{V_1}^{u} = \frac{1}{2\sqrt{2}G_F V_{ub}} \sum_{j,k=1}^{3} \hat{V}_{1k} \frac{\lambda'_{33j}\lambda'^{*}_{3kj}}{2m^2_{\tilde{d}^j_R}}, \quad C_{V_1}^{u\nu_\ell} = \frac{1}{2\sqrt{2}G_F V_{ub}} \sum_{j,k=1}^{3} \hat{V}_{1k} \frac{\lambda'_{\ell 3j}\lambda'^{*}_{3kj}}{2m^2_{\tilde{d}^j_R}}. \quad (145)$$

The Wilson coefficients $C_{V_1}^{c}$ has an allowed region for the results of $\bar{B} \to D^{(*)}\tau\bar{\nu}$ as shown in Fig. 3. The constraint on $C_{V_1}^{u}$ from $\bar{B} \to \tau\bar{\nu}$ is shown in Eq. (85). We can see that the RPV couplings in $C_{V_1}^{c}$ and $C_{V_1}^{u}$ can satisfy requirements for these two constraints at the same time. For illustration purpose to see that, we assume the RPV couplings to be real and define the product of RPV couplings as

$$g_k = \sum_{j=1}^{3} \lambda'_{33j}\lambda'^{*}_{3kj}, \quad (146)$$

assuming $m_{\tilde{d}^j_R} = 500\text{GeV}$. The allowed regions for $C_{V_1}^{c}$ and $C_{V_1}^{u}$ are rewritten as

$$-2.41 < \sum_{k=1}^{3} \hat{V}_{1k} g_k < -2.04, \quad 0.04 < \sum_{k=1}^{3} \hat{V}_{1k} g_k < 0.41, \quad (147)$$

$$-0.75 < \sum_{k=1}^{3} \hat{V}_{2k} g_k < -0.71, \quad 0.03 < \sum_{k=1}^{3} \hat{V}_{2k} g_k < 0.08, \quad (148)$$

in terms of g_k at 90% CL. (We neglect the phase in $\hat{V}_{13} = V_{ub}$ for simplicity.) The conditions in Eqs. (147) and (148) are satisfied as in Fig. 15.

Let us turn and concentrate on another viewpoint. We find that at 90% CL,

$$\left|C_{V_1}^{c}\right| > 0.08, \quad \left|C_{V_1}^{c\nu_\ell}\right| > 0.42, \quad (149)$$

are required to explain the current experimental results of $R(D^{(*)})$. (This means that there is no allowed region within $\left|C_{V_1}^{c}\right| < 0.08$. In other words, it is a necessary condition to explain the data.) The minimal contribution of the RPV couplings, that cause the largest effect on $R(D^{(*)})$, is obtained in the case that the product of RPV couplings for $k = 2$ in $C_{V_1}^{c(\nu_\ell)}$ only contributes to $\bar{B} \to D^{(*)}\tau\bar{\nu}$. In that case, Eq. (149) is converted into

$$|g_2| = \left|\sum_{j=1}^{3} \lambda'_{33j}\lambda'^{*}_{32j}\right| > 0.05, \quad \left|\sum_{j=1}^{3} \lambda'_{\ell 3j}\lambda'^{*}_{32j}\right| > 0.29, \quad (150)$$

assuming $m_{\tilde{d}^j_R} = 500\text{GeV}$. The condition of g_2 in Eq. (150) corresponds to the magenta region with $g_1 = 0$ in Fig. 15. However the same products of RPV couplings as in $C_{V_1}^{c(\nu_\ell)}$ also

contribute to $B \to X_s \nu\bar{\nu}$ [58]. The effective Lagrangian for $b \to s\nu\bar{\nu}$ is generally given by

$$\mathcal{L}_{bs\nu\nu} = \frac{\sqrt{2}\alpha}{\pi} G_F V_{tb} V_{ts}^* \left(C_L^\nu \mathcal{O}_L^\nu + C_R^\nu \mathcal{O}_R^\nu\right) + \text{h.c.}, \tag{151}$$

with the operators

$$\mathcal{O}_L^\nu = s_L \gamma^\mu b_L \, \bar{\nu}_L \gamma_\nu \nu_L, \tag{152}$$

$$\mathcal{O}_R^\nu = s_R \gamma^\mu b_R \, \bar{\nu}_L \gamma_\mu \nu_L. \tag{153}$$

According to Ref. [59], the branching fraction of $B \to X_s \nu\bar{\nu}$ are calculated and estimated as

$$\mathcal{B}(B \to X_s \nu\bar{\nu}) \simeq 2.7 \times 10^{-5} \cdot \frac{|C_L^\nu|^2 + |C_R^\nu|^2}{|(C_L^\nu)^{\text{SM}}|^2}, \tag{154}$$

where $(C_L^\nu)^{\text{SM}}$ is the contribution of the SM, which is calculated as $(C_L^\nu)^{\text{SM}} = -6.38 \pm 0.06$. The relevant Wilson coefficients that come from the RPV interactions in $b \to s\nu_{\ell'}\bar{\nu}_\ell$ are represented as

$$|C_L^\nu|^2 = \frac{1}{3}\sum_{\ell',\ell} |C_L^{\ell'\ell}|^2, \quad |C_R^\nu|^2 = \frac{1}{3}\sum_{\ell',\ell} |C_R^{\ell'\ell}|^2, \tag{155}$$

where

$$C_L^{\ell'\ell} = \tilde{C} \sum_{j=1}^{3} \frac{\lambda'_{\ell 3j} \lambda'^*_{\ell' 2j}}{m^2_{\tilde{d}_R^j}}, \tag{156}$$

$$C_R^{\ell'\ell} = \tilde{C} \sum_{j=1}^{3} \frac{\lambda'_{\ell j 2} \lambda'^*_{\ell' j 3}}{m^2_{\tilde{d}_L^j}}, \tag{157}$$

with

$$\tilde{C} = \frac{\pi}{\sqrt{2}\alpha G_F V_{tb} V_{ts}^*}. \tag{158}$$

The upper limit of the branching ratio is given by

$$\mathcal{B}(B \to X_s \nu\bar{\nu}) < 6.4 \times 10^{-4}, \tag{159}$$

at 90% CL [60], and then according to Eqs. (154) and (159), we get $|C_L^\nu| < 31$. Thus the upper bound on the product of RPV couplings is estimated as

$$\left| \sum_{j=1}^{3} \lambda'_{\ell 3j} \lambda'^*_{\ell' 2j} \right| < 4 \times 10^{-4}, \tag{160}$$

when we assume $m_{\tilde{d}_R^j} = 500\text{GeV}$. We then find that the maximal allowed value for $B \to X_s \nu\bar{\nu}$, which result in Eq. (160), contradicts with the minimal requirement for $\bar{B} \to D^{(*)}\tau\bar{\nu}$ as in Eq. (150).

As a consequence, the product of RPV coupling g_2 is hard to satisfy the constraints from both $\bar{B} \to D^{(*)}\tau\bar{\nu}$ and $B \to X_s\nu\bar{\nu}$. We have the same consequence for the case that $R(D^{(*)})$ and $\mathcal{B}(\bar{B} \to \tau\bar{\nu})$ are explained by g_1 with $g_2 = g_3 = 0$ as seen in Fig. 15. In this case, $|g_1| > 0.12$ is required, but the study from $B \to X_q\nu\bar{\nu}$ implies $\left|\sum_j \lambda'_{\ell 3j}\lambda'^{*}_{\ell' 1j}\right| < O(10^{-4})$ [57]. Thus the RPV interactions g_1 and g_2 cannot explain the results of $\bar{B} \to \tau\bar{\nu}$, $\bar{B} \to D^{(*)}\tau\bar{\nu}$ and $B \to X_q\nu\bar{\nu}$ at the same time. The interaction g_3 does not contribute to $B \to X_q\nu\bar{\nu}$, while the large value is needed for $\bar{B} \to \tau\bar{\nu}$ and $\bar{B} \to D^{(*)}\tau\bar{\nu}$. The possibility for having large value of g_3 in order to explain the results of $\bar{B} \to \tau\bar{\nu}$ and $\bar{B} \to D^{(*)}\tau\bar{\nu}$ is discussed in Ref. [55, 61].

D. Leptoquark models

In the SM, the conservation of the lepton and baryon number is not based on a symmetry but also an incidental issue. In extensions of the SM, a new physics model which violate these conservation is often considered. The MSSM with RPV as shown above is a typical example in this class of model. New particles which mediate quark-lepton transitions can potentially contribute to leptonic quark decays (keeping the lepton and baryon number conservation). Such a particle is called as leptoquark. There are ten independent leptoquarks that respect the symmetry of the SM [62]. The effective Lagrangian with the most general dimensionless couplings of the leptoquarks consists of the following terms:

$$\bar{Q}_L i\sigma_2 e_R S_2, \quad \bar{u}_R L_L S_2, \quad \bar{d}_R L_L S'_2, \tag{161}$$

$$(\bar{Q}^c)_R i\sigma_2 L_L T_1, \quad (\bar{u}^c)_L e_R T_1, \quad (\bar{d}^c)_L e_R T'_1, \tag{162}$$

$$(\bar{Q}^c)_R i\sigma_2 \boldsymbol{\sigma} L_L \mathbf{T_3}, \tag{163}$$

$$\bar{Q}_L \gamma_\mu L_L U_1^\mu, \quad \bar{d}_R \gamma_\mu e_R U_1^\mu, \quad \bar{u}_R \gamma_\mu e_R U_1'^\mu, \tag{164}$$

$$(\bar{Q}^c)_R \boldsymbol{\sigma} \gamma_\mu L_L \mathbf{U_3^\mu}, \tag{165}$$

$$(\bar{d}^c)_L \gamma_\mu L_L V_2^\mu, \quad (\bar{Q}^c)_R \gamma_\mu e_R V_2^\mu, \quad (\bar{u}^c)_L \gamma_\mu L_L V_2'^\mu, \tag{166}$$

and their hermite conjugate, where $S^{(\prime)}, T^{(\prime)}$ and $\mathbf{T}$ are scalar leptoquarks, and $V^{(\prime)}, U^{(\prime)}$ and $\mathbf{U}$ are vector leptoquarks. The subscript of the leptoquarks indicate the dimension of their $SU(2)$ representation. In Table VI, we summarize $SU(3)_c \times SU(2)_W \times U(1)_Y$ quantum numbers of leptoquarks.

	$SU(3)_c$	$SU(2)_W$	$U(1)_Y$
S_2	3	2	7/6
S_2'	3	2	1/6
T_1	3*	1	1/3
T_1'	3*	1	4/3
$\mathbf{T}_3$	3*	3	1/3

	$SU(3)_c$	$SU(2)_W$	$U(1)_Y$
U_1	3	1	2/3
U_1'	3	1	5/3
$\mathbf{U}_3$	3	3	2/3
V_2	3*	2	5/6
V_2'	3*	2	−1/6

TABLE VI: Quantum numbers of leptoquarks.

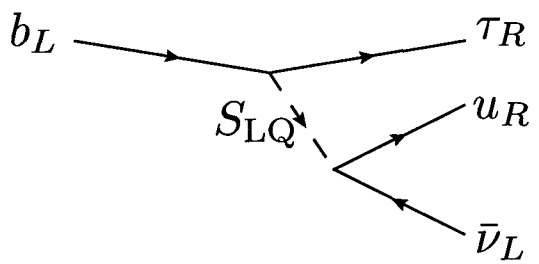

FIG. 16: Scalar leptoquark (represented as S_2) contribution to the decays.

Among them, the following leptoquark model is interesting in the sense that the tensor operator is generated [63],

$$\mathcal{L}_{\rm LQ} = \left(\lambda_{ij}\bar{Q}^i\varepsilon e_R^j + \lambda'_{ij}\bar{u}_R^i L^j\right) S_2, \tag{167}$$

where $\lambda^{(\prime)}$ represents the leptoquark coupling. We show the relevant diagram in Fig. 16 and the effective Lagrangian is represented as

$$\begin{aligned}\mathcal{L}_{\rm eff}^{\rm LQ} &= -\frac{\lambda_{33}^*\lambda'_{i\ell}}{m_{S_{\rm LQ}}^2}\,\bar{\tau}_R b_L\,(\bar{u}_i)_R(\nu_\ell)_L \\ &= \frac{\lambda_{33}^*\lambda'_{i\ell}}{2m_{S_{\rm LQ}}^2}\left((\bar{u}_i)_R b_L\bar{\tau}_R(\nu_\ell)_L + \frac{1}{4}(\bar{u}_i)_R\sigma^{\mu\nu}b_L\bar{\tau}_R\sigma_{\mu\nu}(\nu_\ell)_L\right),\end{aligned} \tag{168}$$

where $m_{S_{\rm LQ}}$ is the scalar leptoquark S_2 mass. Both $\mathcal{O}_{S_2}^{u_i(\nu_\ell)}$ and $\mathcal{O}_T^{u_i(\nu_\ell)}$ appear at the same time, however the Wilson coefficients are related to each other:

$$C_{S_2}^{u_i} = 4C_T^{u_i} = -\frac{1}{2\sqrt{2}G_F\hat{V}_{i3}}\cdot\frac{\lambda_{33}^*\lambda'_{i3}}{2m_{S_{\rm LQ}}^2}, \tag{169}$$

$$C_{S_2}^{u_i\nu_\ell} = 4C_T^{u_i\nu_\ell} = -\frac{1}{2\sqrt{2}G_F\hat{V}_{i3}}\cdot\frac{\lambda_{33}^*\lambda'_{i\ell}}{2m_{S_{\rm LQ}}^2}. \tag{170}$$

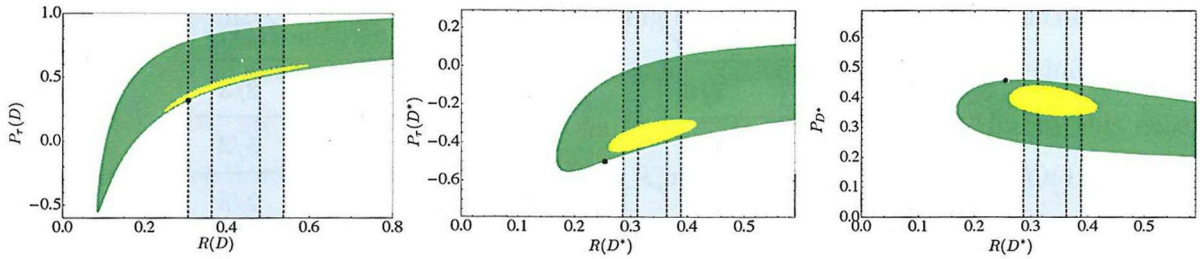

FIG. 17: Correlations between $R(D^{(*)})$ and $P_\tau(D^{(*)})$, and $R(D^*)$ and P_{D^*} in the leptoquark model of Eq. (167) are represented by green regions. Yellow regions indicate the constraints from both the present experimental bounds on $R(D)$ and $R(D^*)$. The black dot in each panel stands for the SM prediction.

In this model, the products of the leptoquark couplings which contribute to $\bar{B} \to \tau\bar{\nu}$ and $\bar{B} \to D^{(*)}\tau\bar{\nu}$ are different[5]. Thus the experimental results of $R(D^{(*)})$ and $\mathcal{B}(\bar{B} \to \tau\bar{\nu})$ give independent bounds on the different leptoquark couplings.

Recollecting that the tensor type operator does not affect $\bar{B} \to \tau\bar{\nu}$ as seen in Sec. II, the situation is the same as the case for $C_{V_1}^u = C_{V_2}^u = C_{S_1}^u = 0$ in Eq. (12). For $\bar{B} \to D^{(*)}\tau\bar{\nu}$, a case that two operators appear in a process at the same time is beyond our analysis in Sec. III. But a similar analysis as the case of one dominant operator can be made since the couplings are related in this model. The right-down panel in Fig. 3 shows the constraint on the above Wilson coefficient $C_{S_2}^c (= 4C_T^c)$. The relevant mass scale of the leptoquark could be of the order of 500GeV:

$$C_{S_2}^c = 4C_T^c \simeq 0.6 \left(\frac{\lambda_{33}^* \lambda'_{23}}{0.4}\right) \left(\frac{500\,\mathrm{GeV}}{m_{S_{\mathrm{LQ}}}}\right)^2 . \tag{171}$$

We find that a rather small new physics contribution $C_{S_2}^c = 4C_T^c \simeq \pm 0.6\,i$ is sufficient to explain the present data compared to the case for only $\mathcal{O}_{S_2}^c$ (The best fit value is $C_{S_2}^c \simeq -1.6$ in this case). In Fig. 17, we show the correlations between decay rates and polarizations in the above leptoquark model. The green regions represent the correlations, $R(D^{(*)})$–$P_\tau(D^{(*)})$ and $R(D^*)$–P_{D^*}, as in Fig. 7. Taking into account both the experimental constraints on $R(D)$ and $R(D^*)$ at the same time, we find the present allowed regions at 99% CL as shown by the yellow regions.

[5] In the mass basis, the flavor mixing matrix like as the CKM matrix enters in the Lagrangian. In the case we consider here, such a matrix can be absorbed into the redefinition of $\lambda_{ij}^{(\prime)}$.

VII. SUMMARY AND CONCLUSION

We have studied the exclusive pure- and semi-tauonic B decays, $\bar{B} \to \tau\bar{\nu}$ and $\bar{B} \to D^{(*)}\tau\bar{\nu}$, in the model-independent manner based on the effective Lagrangian including all the possible four-Fermi operators. For the study from $\bar{B} \to \tau\bar{\nu}$, we have seen that the Wilson coefficients coming from new physics operators are suppressed. In particular the scalar type interactions $C^u_{S_{1,2}}$ are rather constrained due to the enhancement factor. For the study from $\bar{B} \to D^{(*)}\tau\bar{\nu}$, it has turned out that the current experimental values of $R(D^{(*)})$ are not explained by the operator $\mathcal{O}^{c(\nu_\ell)}_{S_1}$ nor $\mathcal{O}^{c\nu_\ell}_{S_2}$ alone while the other operators $\mathcal{O}^c_{S_2}$, $\mathcal{O}^{c(\nu_\ell)}_{V_1}$, $\mathcal{O}^{c(\nu_\ell)}_{V_2}$, and $\mathcal{O}^{c(\nu_\ell)}_T$ reasonably work under the assumption of one-operator dominance.

More precise data that will be given in a future super B factory experiment will allow us to identify the relevant new physics operator among these operators if the deviation from the SM persists. In addition, a lot of data will also allow us to measure the longitudinal tau and D^* polarizations. We have studied the new physics effect on these quantities and estimated their statistical sensitivities to be measured. We have pointed out that correlations among observables including the decay rates, the polarizations and q^2 distributions are useful to distinguish the relevant operator from irrelevant one in new physics.

Furthermore, we have studied several interesting models that contribute to $R(D^{(*)})$ and $\mathcal{B}(\bar{B} \to \tau\bar{\nu})$ based on our model-independent analysis. In 2HDMs without tree-level FCNC and MSSM, only $O^{u,c}_{S_1}$ could be enhanced and thus are unlikely to explain the deviations of $R(D^{(*)})$ form the SM. Our combined fit to the parameter in the 2HDM of type II suggest that this model is excluded with more than 99.9% confidence level.

While the contribution of $O^c_{S_2}$, generated in 2HDMs of type II and type X with FCNC, could be sizable keeping the small contribution of $\mathcal{O}^u_{S_2}$ to $\bar{B} \to \tau\bar{\nu}$. The above situation depends on the magnitude of the $t \to c$ FCNC parameter, which induce direct FCNC top quark decay such as $t \to ch$. We have found that the branching ratio of $t \to ch$ turns out to be at most 12% of the top main decay $t \to bW$ when the experimental values of $R(D^{(*)})$ are obtained by the contribution of the charged Higgs boson in the 2HDMs of type II and type X with FCNC. If this is the case, top decays might be more important for the ILC and LHC experiments.

The MSSM with R-parity violation generates the operators $\mathcal{O}^q_{S_1}$ and $\mathcal{O}^q_{V_1}$ and then contribute to $\bar{B} \to \tau\bar{\nu}$ and $\bar{B} \to D^{(*)}\tau\bar{\nu}$. We have seen that the interactions that enter these B

meson decays are related to each other via the CKM matrix. The combined fit to the RPV couplings in $\mathcal{O}^q_{S_1}$ gives the same consequence as the 2HDMs without FCNC. The parameter region that explains both $R(D^{(*)})$ and $\mathcal{B}(\bar{B} \to \tau\bar{\nu})$ exists in $\mathcal{O}^q_{V_1}$. However we have pointed out that this allowed region is inconsistent with the experimental bound on $B \to X_s\nu\bar{\nu}$.

The interactions that mediate leptoquarks potentially affect leptonic quark decays. Among them, we have focused on the scalar leptoquark model that simultaneously induces $O^q_{S_2}$ and O^q_T. This model is beyond our assumption which is imposed in model-independent analysis. Then we have re-evaluated the constraint on the Wilson coefficient, the effect on polarizations and correlations. We have seen that this model describes the data with a relatively small Wilson coefficient in both $\bar{B} \to \tau\bar{\nu}$ and $\bar{B} \to D^{(*)}\tau\bar{\nu}$ compared to the case only for $O^q_{S_2}$.

The conclusion is as follows. Both the decays $\bar{B} \to \tau\bar{\nu}$ and $\bar{B} \to D^{(*)}\tau\bar{\nu}$ are powerful tools to explore new physics in the charged current. Since these decays are often related in new physics models, it is important to study their combinations. The semi-tauonic decays have advantages to provide a wide variety of observables besides the branching fraction, such as polarizations. These observables, including q^2 distributions, are quite useful in order to clarify possible new physics model-independently. The model-independent analysis allow us to see the new physics features in the decays, while the fit to the specified model parameter gives the concrete bound on new physics model.

Acknowledgments

I am very grateful to Minoru Tanaka for his great advises, encouragements, stimulating discussions and collaborations. I am very grateful to my supervisor Prof. Tetsuya Onogi for various supports and encouragements. I would like to thank Andrey Tayduganov for useful comments and discussions. Finally, I thank all members of particle physics theory group at Osaka University. This work is supported in part by the Grant-in-Aid for Science Research, Ministry of Education, Culture, Sports, Science and Technology, Japan, under Grant No. 248920.

APPENDIX A: COMBINATION OF MEASUREMENTS

Here we show the way to combine two independent measurements assuming the gaussian distribution. Suppose that $x_i \pm \delta x_i$, $y_i \pm \delta y_i$ and ρ_i are the measurements of x, y including the errors and their correlation, which are obtained at the experiment i. In this case, χ^2 distribution of the quantities x and y is represented as

$$\chi_i^2 = \frac{1}{1-\rho_i^2}\left[\frac{(x-x_i)^2}{\delta x_i^2} + \frac{(y-y_i)^2}{\delta y_i^2} - \frac{2\rho_i(x-x_i)(y-y_i)}{\delta x_i \delta y_i}\right]. \tag{A1}$$

When the two independent experiments A and B observed x, y and obtained their values, the combined measurements are derived from the sum of χ^2 distribution:

$$\chi_A^2 + \chi_B^2 = \chi_C^2, \tag{A2}$$

where C indicates the combined result. The central values x_C, y_C, their errors $\delta x_C, \delta y_C$ and the correlation ρ_C are written as

$$x_C = \delta x_C^2 \, Z_x + \rho_C \, \delta x_C \, \delta y_C \, Z_y, \tag{A3}$$

$$y_C = \delta y_C^2 \, Z_y + \rho_C \, \delta x_C \, \delta y_C \, Z_x, \tag{A4}$$

with

$$\delta x_C = \frac{W_y}{W_x W_y - W_{xy}^2}, \tag{A5}$$

$$\delta y_C = \frac{W_x}{W_x W_y - W_{xy}^2}, \tag{A6}$$

$$\rho_C = \frac{W_{xy}}{\sqrt{W_x W_y}}, \tag{A7}$$

where W and Z are represented as

$$W_x = \sum_i \frac{1}{(1-\rho_i^2)\delta x_i^2}, \quad W_y = \sum_i \frac{1}{(1-\rho_i^2)\delta y_i^2}, \quad W_{xy} = \sum_i \frac{\rho_i}{(1-\rho_i^2)\delta x_i \delta y_i}, \tag{A8}$$

$$Z_x = \sum_i \left[\frac{x_i}{(1-\rho_i^2)\delta x_i^2} - \frac{\rho_i y_i}{(1-\rho_i^2)\delta x_i \delta y_i}\right], \; Z_y = \sum_i \left[\frac{y_i}{(1-\rho_i^2)\delta y_i^2} - \frac{\rho_i x_i}{(1-\rho_i^2)\delta x_i \delta y_i}\right]. \tag{A9}$$

APPENDIX B: FORM FACTORS

Here we derive consistent definitions of form factors. In order to know the correct forms of the amplitudes, it is helpful to write down the properties of the parity $\mathcal{P}$ and time-reversal $\mathcal{T}$

transformations in $\bar{B} \to D^{(*)}$ transitions. For the meson states, the parity transformations are written as

$$\mathcal{P}\left|\bar{B}(p_B)\right\rangle = -\left|\bar{B}(p'_B)\right\rangle, \tag{B1}$$

$$\mathcal{P}\left|D(p_D)\right\rangle = -\left|D(p'_D)\right\rangle, \tag{B2}$$

$$\mathcal{P}\left|D^*(p_D,\epsilon)\right\rangle = \left|D^*(p'_D,\epsilon')\right\rangle, \tag{B3}$$

where $p = (p_0, \mathbf{p})$ and $p' = (p_0, -\mathbf{p})$. We choose the time-reversal transformations [6] as follows:

$$\mathcal{T}\left|\bar{B}(p_B)\right\rangle = +\left|\bar{B}(p'_B)\right\rangle, \tag{B4}$$

$$\mathcal{T}\left|D(p_D)\right\rangle = +\left|D(p'_D)\right\rangle, \tag{B5}$$

$$\mathcal{T}\left|D^*(p_D,\epsilon)\right\rangle = \left|D^*(p'_D,\epsilon')\right\rangle. \tag{B6}$$

Then we see the following relations:

$$\left\langle D(p_D)\left|\,\bar{c}b\,\right|\bar{B}(p_B)\right\rangle = \left\langle D(p'_D)\left|\,\bar{c}b\,\right|\bar{B}(p'_B)\right\rangle, \tag{B7}$$

$$\left\langle D(p_D)\left|\,\bar{c}\gamma^\mu b\,\right|\bar{B}(p_B)\right\rangle = (-1)^\mu\left\langle D(p'_D)\left|\,\bar{c}\gamma^\mu b\,\right|\bar{B}(p'_B)\right\rangle, \tag{B8}$$

$$\left\langle D(p_D)\left|\,\bar{c}\sigma^{\mu\nu} b\,\right|\bar{B}(p_B)\right\rangle = (-1)^\mu(-1)^\nu\left\langle D(p'_D)\left|\,\bar{c}\sigma^{\mu\nu} b\,\right|\bar{B}(p'_B)\right\rangle, \tag{B9}$$

$$\left\langle D^*(p_D,\epsilon)\left|\,\bar{c}b\,\right|\bar{B}(p_B)\right\rangle = (-1)\left\langle D^*(p'_D,\epsilon')\left|\,\bar{c}b\,\right|\bar{B}(p'_B)\right\rangle, \tag{B10}$$

$$\left\langle D^*(p_D,\epsilon)\left|\,\bar{c}\gamma^5 b\,\right|\bar{B}(p_B)\right\rangle = \left\langle D^*(p'_D,\epsilon')\left|\,\bar{c}\gamma^5 b\,\right|\bar{B}(p'_B)\right\rangle, \tag{B11}$$

$$\left\langle D^*(p_D,\epsilon)\left|\,\bar{c}\gamma^\mu b\,\right|\bar{B}(p_B)\right\rangle = (-1)(-1)^\mu\left\langle D^*(p'_D,\epsilon')\left|\,\bar{c}\gamma^\mu b\,\right|\bar{B}(p'_B)\right\rangle, \tag{B12}$$

$$\left\langle D^*(p_D,\epsilon)\left|\,\bar{c}\gamma^\mu\gamma^5 b\,\right|\bar{B}(p_B)\right\rangle = (-1)^\mu\left\langle D^*(p'_D,\epsilon')\left|\,\bar{c}\gamma^\mu\gamma^5 b\,\right|\bar{B}(p'_B)\right\rangle, \tag{B13}$$

$$\left\langle D^*(p_D,\epsilon)\left|\,\bar{c}\sigma^{\mu\nu} b\,\right|\bar{B}(p_B)\right\rangle = (-1)(-1)^\mu(-1)^\nu\left\langle D^*(p'_D,\epsilon')\left|\,\bar{c}\sigma^{\mu\nu} b\,\right|\bar{B}(p'_B)\right\rangle, \tag{B14}$$

[6] Depending on a choice of phase, we can select and define reasonable form factors.

where $(-1)^0 = 1$ and $(-1)^i = -1$ for parity transformations, and

$$\langle D(p_D) \,|\, \bar{c}b \,|\, \bar{B}(p_B)\rangle = \langle D(p'_D) \,|\, \bar{c}b \,|\, \bar{B}(p'_B)\rangle^* , \tag{B15}$$

$$\langle D(p_D) \,|\, \bar{c}\gamma^\mu b \,|\, \bar{B}(p_B)\rangle = (-1)^\mu \langle D(p'_D) \,|\, \bar{c}\gamma^\mu b \,|\, \bar{B}(p'_B)\rangle^* , \tag{B16}$$

$$\langle D(p_D) \,|\, \bar{c}\sigma^{\mu\nu} b \,|\, \bar{B}(p_B)\rangle = (-1)(-1)^\mu(-1)^\nu \langle D(p'_D) \,|\, \bar{c}\sigma^{\mu\nu} b \,|\, \bar{B}(p'_B)\rangle^* , \tag{B17}$$

$$\langle D^*(p_D,\epsilon) \,|\, \bar{c}b \,|\, \bar{B}(p_B)\rangle = \langle D^*(p'_D,\epsilon') \,|\, \bar{c}b \,|\, \bar{B}(p'_B)\rangle^* , \tag{B18}$$

$$\langle D^*(p_D,\epsilon) \,|\, \bar{c}\gamma^5 b \,|\, \bar{B}(p_B)\rangle = \langle D^*(p'_D,\epsilon') \,|\, \bar{c}\gamma^5 b \,|\, \bar{B}(p'_B)\rangle^* , \tag{B19}$$

$$\langle D^*(p_D,\epsilon) \,|\, \bar{c}\gamma^\mu b \,|\, \bar{B}(p_B)\rangle = (-1)^\mu \langle D^*(p'_D,\epsilon') \,|\, \bar{c}\gamma^\mu b \,|\, \bar{B}(p'_B)\rangle^* , \tag{B20}$$

$$\langle D^*(p_D,\epsilon) \,|\, \bar{c}\gamma^\mu\gamma^5 b \,|\, \bar{B}(p_B)\rangle = (-1)^\mu \langle D^*(p'_D,\epsilon') \,|\, \bar{c}\gamma^\mu\gamma^5 b \,|\, \bar{B}(p'_B)\rangle^* , \tag{B21}$$

$$\langle D^*(p_D,\epsilon) \,|\, \bar{c}\sigma^{\mu\nu} b \,|\, \bar{B}(p_B)\rangle = (-1)(-1)^\mu(-1)^\nu \langle D^*(p'_D,\epsilon') \,|\, \bar{c}\sigma^{\mu\nu} b \,|\, \bar{B}(p'_B)\rangle^* , \tag{B22}$$

for time-reversal transformations. Due to these properties in the strong interactions, one find that $\bar{B} \to D^{(*)}$ amplitudes take the following forms:

$$\langle D(p_D) \,|\, \bar{c}\gamma^\mu b \,|\, \bar{B}(p_B)\rangle = \sqrt{m_B m_D}\,[h_+(w)(v+v')^\mu + h_-(w)(v-v')^\mu], \tag{B23}$$

$$\langle D(p_D) \,|\, \bar{c}b \,|\, \bar{B}(p_B)\rangle = \sqrt{m_B m_D}(w+1)h_S(w), \tag{B24}$$

$$\langle D(p_D) \,|\, \bar{c}\sigma^{\mu\nu} b \,|\, \bar{B}(p_B)\rangle = -i\sqrt{m_B m_D}h_T(w)(v^\mu v'^\nu - v^\nu v'^\mu), \tag{B25}$$

$$\langle D^*(p_D,\epsilon) \,|\, \bar{c}\gamma^\mu b \,|\, \bar{B}(p_B)\rangle = i\sqrt{m_B m_{D^*}}h_V(w)\varepsilon^{\mu\nu\rho\sigma}\epsilon^*_\nu v'_\rho v_\sigma, \tag{B26}$$

$$\begin{aligned}\langle D^*(p_D,\epsilon) \,|\, \bar{c}\gamma^\mu\gamma^5 b \,|\, \bar{B}(p_B)\rangle = {} & \sqrt{m_B m_{D^*}}\Big[h_{A_1}(w)(w+1)\epsilon^{*\mu} \\ & -h_{A_2}(w)(\epsilon^*\cdot v)v^\mu - h_{A_3}(w)(\epsilon^*\cdot v)v'^\mu\Big],\end{aligned} \tag{B27}$$

$$\langle D^*(p_D,\epsilon) \,|\, \bar{c}\gamma^5 b \,|\, \bar{B}(p_B)\rangle = -\sqrt{m_B m_{D^*}}\,(\epsilon^*\cdot v)h_P(w), \tag{B28}$$

$$\begin{aligned}\langle D^*(p_D,\epsilon) \,|\, \bar{c}\sigma^{\mu\nu} b \,|\, \bar{B}(p_B)\rangle = {} & -\sqrt{m_B m_{D^*}}\,\varepsilon^{\mu\nu\rho\sigma}\Big[h_{T_1}(w)\epsilon^*_\rho(v+v')_\sigma \\ & +h_{T_2}(w)\epsilon^*_\rho(v-v')_\sigma \\ & +h_{T_3}(w)(\epsilon^*\cdot v)(v+v')_\rho(v-v')_\sigma\Big],\end{aligned} \tag{B29}$$

where $v^\mu = p_B^\mu/m_B$, $v'^\mu = p_M^\mu/m_M$, $w = v\cdot v'$ and $\varepsilon^{0123} = -1$. The amplitudes corresponding to the operator $\bar{c}\sigma^{\mu\nu}\gamma_5 b$ are given by the following identity,

$$\sigma^{\mu\nu}\gamma_5 = -\frac{i}{2}\varepsilon^{\mu\nu\alpha\beta}\sigma_{\alpha\beta}\,. \tag{B30}$$

APPENDIX C: HEAVY QUARK EFFECTIVE THEORY

Here we briefly review the heavy quark effective theory (HQET). HQET is a useful approximation to treat the hadronic matrix element in the presence of a heavy quark.

1. Heavy quark limit

We consider a heavy quark field Q with its mass to be m_Q. We define the four momentum of Q as

$$p^\mu = m_Q v^\mu + k^\mu, \tag{C1}$$

where $v^2 = 1$ and k is a residual momentum which determines a scale of interaction of off-shell quark Q. For heavy quarks in hadron, k is the oder of $\Lambda_{\rm QCD}$. Suppose Q is divided into two fields Q_v^l and Q_v^h as follows:

$$Q(x) = e^{-im_Q v\cdot x}\left(Q_v^l(x) + Q_v^h(x)\right), \tag{C2}$$

where

$$Q_v^l(x) = e^{im_Q v\cdot x}\frac{1+\not{v}}{2}Q(x), \quad Q_v^h(x) = e^{im_Q v\cdot x}\frac{1-\not{v}}{2}Q(x). \tag{C3}$$

Using these representations, QCD Lagrangian of the quark field Q is written as

$$\begin{aligned}\mathcal{L}_{\rm QCD} &= \bar{Q}(i\not{D} - m_Q)Q \\ &= \bar{Q}_v^l(iv\cdot D)Q_v^l - \bar{Q}_v^h(iv\cdot D + 2m_Q)Q_v^h + \bar{Q}_v^l(i\not{D})Q_v^h + \bar{Q}_v^h(i\not{D})Q_v^l,\end{aligned} \tag{C4}$$

where $D_\mu = \partial_\mu + igt^aG_\mu^a$ is the QCD gauge covariant derivative. As seen in the first term of Eq. (C4), the field Q_v^l describes mass-independent part of Q. From Eq. (C4), the equation of motion is represented as

$$(iv\cdot D + 2m_Q)Q_v^h = (i\not{D}_\perp)Q_v^l, \tag{C5}$$

where $D_\perp^\mu = D^\mu - (D\cdot v)v^\mu$. When we integrate out Q_v^h using Eq. (C5), we can represent the heavy quark field Q and QCD Lagrangian $\mathcal{L}_{\rm QCD}$ as

$$Q(x) = e^{-im_Q v\cdot x}\left(1 + \frac{i\not{D}_\perp}{iv\cdot D + 2m_Q}\right)Q_v^l(x), \tag{C6}$$

$$\mathcal{L}_{\rm QCD} = \bar{Q}_v^l\left(iv\cdot D + (i\not{D}_\perp)\frac{1}{iv\cdot D + 2m_Q}(i\not{D}_\perp)\right)Q_v^l. \tag{C7}$$

In the limit $m_Q \to \infty$, which is referred as heavy quark limit (HQL), $\mathcal{L}_{\rm QCD}$ turns out to be

$$\mathcal{L}^{(0)}_{\rm HQET} = \bar{Q}^l_v (iv \cdot D) Q^l_v. \tag{C8}$$

Therefore, the QCD Lagrangian for the heavy quark field Q in the HQL is mass-independent and thus has the flavor and spin symmetry. Since $Q(x) = e^{-im_Q v\cdot x} Q^l_v(x)$ in the HQL, we see the following relation,

$$\bar{Q}\gamma^\mu Q = \bar{Q}^l_v \gamma^\mu Q^l_v = \bar{Q}^l_v v^\mu Q^l_v. \tag{C9}$$

Thus the effective Lagrangian $\mathcal{L}^{(0)}_{\rm HQET}$ generates the same quark propagator and QCD vertex as the full QCD Lagrangian at the leading order in $1/m_Q$ and $\alpha_s(m_Q)$.

2. Classification and representation of mesons

As seen above, a heavy quark has a spin symmetry in the HQL. Thus a total angular momentum $\mathbf{J}$ of a hadron which contains a heavy quark can be divided into two conserved spins $\mathbf{S}_Q, \mathbf{S}_\ell$ so as to $\mathbf{J} = \mathbf{S}_Q + \mathbf{S}_\ell$, where $\mathbf{S}_Q$ indicates a spin of heavy quark and $\mathbf{S}_\ell$ represents a spin of light degrees of freedom. We define these quantum numbers as $\mathbf{J}^2 = j(j+1), \mathbf{S}^2_Q = s_Q(s_Q+1)$ and $\mathbf{S}^2_\ell = s_\ell(s_\ell+1)$. Ground state mesons containing a heavy quark Q are composed of a heavy quark with $s_Q = 1/2$ and some light degrees of freedom (effectively to be light antiquark $\bar{q}$) with $s_\ell = 1/2$. Therefore they form a multiplet of mesons with total angular momentum $j = 1/2 \otimes 1/2 = 0 \oplus 1$ and their parity $p = -1$.

We define the corresponding pseudo-scalar ($j^p = 0^-$) and vector ($j^p = 1^-$) meson field operators as P^Q_v and $P^{*Q}_{v\mu}$, respectively. For example, the fields P^c_v and P^{*c}_v indicate D and D^* mesons respectively. The meson fields P^Q_v and $P^{*Q}_{v\mu}$ should be represented as a single field H^Q_v because they belong to the same multiplet. The simple and consistent definition turns out to be

$$H^Q_v = \frac{1+\not{v}}{2}\left(\not{P}^{*Q}_v - \gamma^5 P^Q_v\right). \tag{C10}$$

The projective operator $(1+\not{v})/2$ retains only the particle component of the heavy quark field Q. The conjugate field of H^Q_v is expressed as

$$\bar{H}^Q_v = \gamma^0 H^{Q\dagger}_v \gamma^0 = \left(P^{*Q\dagger}_{v\mu}\gamma^\mu + P^{Q\dagger}_v \gamma^5\right)\frac{1+\not{v}}{2}. \tag{C11}$$

The relative phase between the first and second terms in Eq. (C10) depends on the definition of the meson states as shown later.

3. Hadronic matrix element in HQET : leading order

From here, we concentrate on the transition from the $\bar{B}$ meson to the D or D^* mesons. $\bar{B} \to D^{(*)}$ transition consists of the quark current $\bar{c}\,\Gamma\, b$ where $\Gamma = \gamma^\mu$ or $\gamma^\mu\gamma^5$ in SM and the others $\Gamma = \mathbf{1}, \gamma^5, \sigma^{\mu\nu}$ may appear in new physics models. Since the b and c quarks have the heavy masses m_b and m_c respectively, the corresponding fields are defined as b_v and $c_{v'}$ in the HQET. Similarly to Eq. (C9),

$$\bar{c}\,\Gamma\, b = \bar{c}_{v'}\,\Gamma\, b_v, \tag{C12}$$

in the HQL. In order to evaluate the hadronic matrix element $\langle D^{(*)}(p')|\bar{c}\,\Gamma\, b|\bar{B}(p)\rangle$, we should relate $\bar{c}_{v'}\,\Gamma\, b_v$ as the meson covariant fields H_v^b and $H_{v'}^c$. Lorenz covariance and heavy quark spin transformation require the following representation:

$$\bar{c}_{v'}\,\Gamma\, b_v = \mathrm{Tr}\left(X(w)\bar{H}_{v'}^c \Gamma H_v^b\right), \tag{C13}$$

where $w = v\cdot v'$ and $X(w) = X_0(w) + X_1(w)\not{v} + X_2(w)\not{v}' + X_3(w)\not{v}\not{v}'$ is the most general form. Using the properties such as

$$\not{v} H_v^Q = H_v^Q, \quad H_v^Q \not{v} = -H_v^Q, \quad \not{v}\bar{H}_v^Q = -\bar{H}_v^Q, \quad \bar{H}_v^Q \not{v} = \bar{H}_v^Q, \tag{C14}$$

we can rewrite Eq. (C13) into the following form:

$$\bar{c}_{v'}\,\Gamma\, b_v = (X_0 - X_1 - X_2 + X_3)\mathrm{Tr}\left(\bar{H}_{v'}^c \Gamma H_v^b\right) \equiv -\xi(w)\mathrm{Tr}\left(\bar{H}_{v'}^c \Gamma H_v^b\right), \tag{C15}$$

where $\xi(w)$ is called as Isgur-Wise function [32]. Then the hadronic matrix elements are represented as

$$\langle D(v')|\,\bar{c}_{v'}\gamma_\mu b_v\,|\bar{B}(v)\rangle = \xi(w)\left(v_\mu + v'_\mu\right), \tag{C16}$$

$$\langle D(v')|\,\bar{c}_{v'}\gamma_\mu\gamma^5 b_v\,|\bar{B}(v)\rangle = 0, \tag{C17}$$

$$\langle D(v')|\,\bar{c}_{v'} b_v\,|\bar{B}(v)\rangle = \xi(w)(1+w), \tag{C18}$$

$$\langle D(v')|\,\bar{c}_{v'}\gamma^5 b_v\,|\bar{B}(v)\rangle = 0, \tag{C19}$$

$$\langle D(v')|\,\bar{c}_{v'}\sigma_{\mu\nu} b_v\,|\bar{B}(v)\rangle = i\xi(w)\left(v'_\mu v_\nu - v'_\nu v_\mu\right), \tag{C20}$$

$$\langle D(v')|\,\bar{c}_{v'}\sigma_{\mu\nu}\gamma^5 b_v\,|\bar{B}(v)\rangle = \xi(w)\varepsilon_{\mu\nu\alpha\beta}\, v^\alpha v'^\beta, \tag{C21}$$

for $\bar{B} \to D$ transitions and

$$\langle D^*(v',\epsilon)|\,\bar{c}_{v'}\gamma_\mu b_v\,|\bar{B}(v)\rangle = \xi(w)\varepsilon_{\mu\nu\alpha\beta}\,\epsilon^{*\nu}v'^{\alpha}v^{\beta}, \tag{C22}$$

$$\langle D^*(v',\epsilon)|\,\bar{c}_{v'}\gamma_\mu\gamma_5 b_v\,|\bar{B}(v)\rangle = -i\xi(w)\left[(1+w)\epsilon^*_\mu - (\epsilon^*\cdot v)\,v'_\mu\right], \tag{C23}$$

$$\langle D^*(v',\epsilon)|\,\bar{c}_{v'}b_v\,|\bar{B}(v)\rangle = 0, \tag{C24}$$

$$\langle D^*(v',\epsilon)|\,\bar{c}_{v'}\gamma_5 b_v\,|\bar{B}(v)\rangle = -\xi(w)\,(\epsilon^*\cdot v), \tag{C25}$$

$$\langle D^*(v',\epsilon)|\,\bar{c}_{v'}\sigma_{\mu\nu} b_v\,|\bar{B}(v)\rangle = \xi(w)\varepsilon_{\mu\nu\alpha\beta}\,\epsilon^{*\alpha}\,(v'+v)^{\beta}, \tag{C26}$$

$$\langle D^*(v',\epsilon)|\,\bar{c}_{v'}\sigma_{\mu\nu}\gamma_5 b_v\,|\bar{B}(v)\rangle = -i\xi(w)\left[\epsilon^*_\mu\,(v'+v)_\nu - \epsilon^*_\nu\,(v'+v)_\mu\right], \tag{C27}$$

for $\bar{B} \to D^*$ transitions, where ϵ indicates a polarization vector of D^* meson and we define the normalization for hadronic state in HQET as

$$\langle H(v',k')|H(v,k)\rangle = 2v^0\delta_{vv'}(2\pi)^3\delta^3(\mathbf{k}'-\mathbf{k}). \tag{C28}$$

As seen in these results, the heavy quark symmetry implies that $\bar{B} \to D$ and $\bar{B} \to D^*$ transitions induced by any currents $\bar{c}\,\Gamma\,b$ are parametrized as a common variable $\xi(w)$. In addition, we see $\xi(1) = 1$ from the heavy quark flavor symmetry.

4. Radiative corrections : $\alpha_s(m_Q)$ expansion

In general, a renormalization of an effective field differs from that of its original filed. Thus we must take into account such a difference as a radiative correction in the effective theory. This procedure is often called as matching between a full theory and an effective theory. Here we briefly review the matching of $b \to c$ currents between QCD and HQET. By means of HQET operators, the QCD currents $\bar{c}\gamma^\mu b$ and $\bar{c}\gamma^\mu\gamma^5 b$ are represented as

$$\bar{c}\gamma^\mu b = C_1^V(\mu)\,\bar{c}_{v'}\gamma^\mu b_v + C_2^V(\mu)\,\bar{c}_{v'}v^\mu b_v + C_3^V(\mu)\,\bar{c}_{v'}v'^\mu b_v, \tag{C29}$$

$$\bar{c}\gamma^\mu\gamma^5 b = C_1^A(\mu)\,\bar{c}_{v'}\gamma^\mu\gamma^5 b_v + C_2^A(\mu)\,i\bar{c}_{v'}v^\mu\gamma^5 b_v + C_3^A(\mu)\,i\bar{c}_{v'}v'^\mu\gamma^5 b_v, \tag{C30}$$

where $C_i^{V,A}$ are Wilson coefficients which include effects of radiative corrections and μ indicates a renormalization scale. The operators in HQET also depend on the renormalization scale but we omit its label. The right-hand sides of these relations include all dimension three operators with the same quantum numbers as $\bar{c}\,\gamma^\mu\,b$ and $\bar{c}\,\gamma^\mu\gamma^5\,b$. These are the relations at the HQL and higher dimension operators emerge at and after the NLO of $1/m_Q$ expansion. Here we review the matching at the HQL.

The HQET is constructed to reproduce correctly the low momentum behavior of the full QCD but cannot describe the physics at a high momentum scale $\mu > m_Q$. Thus the computation of the matching is perturbatively done at the scale $\mu = m_Q$. In actual $b \to c$ transition case, the matching scale is chosen to be $\mu = \sqrt{m_b m_c} \equiv \bar{m}$, which means that the transition to HQET is made simultaneously for both b and c quarks. [7] At lowest order in $\alpha_s(\bar{m})$ expansion, the matching condition is trivially,

$$C_1^V(\bar{m}) = 1 + O(\alpha_s(\bar{m})), \quad C_2^V(\bar{m}) = O(\alpha_s(\bar{m})), \quad C_3^V(\bar{m}) = O(\alpha_s(\bar{m})), \tag{C31}$$

$$C_1^A(\bar{m}) = 1 + O(\alpha_s(\bar{m})), \quad C_2^A(\bar{m}) = O(\alpha_s(\bar{m})), \quad C_3^A(\bar{m}) = O(\alpha_s(\bar{m})). \tag{C32}$$

The radiative correction at a low momentum scale ($\mu < \bar{m}$) is obtained by renormalization group equations. When we consider such a correction, the relation between the heavy quark field and the covariant representation of meson field in Eq. (C15) has to be redefined as

$$\bar{c}_{v'} \Gamma b_v \equiv -\xi(w,\mu) \mathrm{Tr}\left(\bar{H}^c_{v'} \Gamma H^b_v\right), \tag{C33}$$

since the operators in the HQET depend on a renormalization scale μ as stated above. Thus the matrix elements for the physical transitions $\bar{B} \to D^{(*)}$ are represented as

$$\begin{aligned}
\langle D(v')|\, \bar{c}\gamma_\mu b\, |\bar{B}(v)\rangle &= \left[C_1^V(\mu) - \frac{w+1}{2}(C_2^V(\mu) + C_3^V(\mu))\right] \xi(w,\mu)(v_\mu + v'_\mu) \\
&\quad + \frac{w+1}{2}(C_3^V(\mu) - C_2^V(\mu))\xi(w,\mu)(v_\mu - v'_\mu), \qquad \text{(C34)} \\
\langle D^*(v',\epsilon)|\, \bar{c}\gamma_\mu b\, |\bar{B}(v)\rangle &= C_1^V(\mu)\xi(w,\mu)\varepsilon_{\mu\nu\alpha\beta}\, \epsilon^{*\nu} v'^{\alpha} v^{\beta}, \qquad \text{(C35)} \\
\langle D^*(v',\epsilon)|\, \bar{c}\gamma_\mu\gamma^5 b\, |\bar{B}(v)\rangle &= -iC_1^A(\mu)\xi(w,\mu)(1+w)\epsilon^*_\mu - iC_2^A(\mu)\xi(w,\mu)\,(\epsilon^* \cdot v)\, v_\mu \\
&\quad + i\left(C_1^A(\mu) - C_3^A(\mu)\right)\xi(w,\mu)\,(\epsilon^* \cdot v)\, v'_\mu. \qquad \text{(C36)}
\end{aligned}$$

Since the physical transitions do not depend on a scale μ, we can redefine the product $C_i^{V,A}(\mu)\xi(w,\mu)$ so as to

$$C_i^{V,A}(\mu)\xi(w,\mu) \equiv \hat{C}_i^{V,A}\hat{\xi}(w), \tag{C37}$$

where $\hat{C}_i^{V,A}$ and $\hat{\xi}(w)$ indicate μ independent renormalized Wilson coefficient and Isgur-Wise function respectively. According to Ref.[11], the coefficients $\hat{C}_i^{V,A}$ determined by renormal-

[7] We can consider two different transition scales for b and c quarks in general. For example, see Ref.[64].

ization group scaling from $\bar{m}$ take the following forms:

$$\hat{C}_1^{V/A} = A(w)\Bigg(1+\frac{\alpha_s(m_b)-\alpha_s(m_c)}{\pi}\delta'_Z+\frac{2\alpha_s(\bar{m})}{3\pi}g(z,w) + \frac{\alpha_s(m_c)}{\pi}\left[Z(w)+\frac{2}{3}\big(f(w)\pm r(w)\big)\right]\Bigg), \tag{C38}$$

$$\hat{C}_2^{V/A} = A(w)\left(\pm\frac{2\alpha_s(m_b)}{3\pi}-\frac{4\alpha_s(m_c)}{3\pi}r(w)-\frac{2\alpha_s(\bar{m})}{3\pi}h_1(z,w)\right), \tag{C39}$$

$$\hat{C}_3^{V/A} = \mp A(w)\frac{2\alpha_s(\bar{m})}{3\pi}h_2(z,w), \tag{C40}$$

where the above functions are defined in Ref.[11]. The factor $A(w)$ stands for the leading logarithmic scaling effect.

5. Nonperturbative corrections : $1/m_Q$ expansion

In turn, we consider the hadronic matrix element including $1/m_Q$ correction. Expanding Eq. (C6) by $1/m_Q$, we obtain

$$Q(x) = e^{-im_Q v\cdot x}\left(1+i\frac{\not{D}_\perp}{2m_Q}+O\left(\frac{1}{m_Q^2}\right)\right)Q_v^l(x). \tag{C41}$$

For $b\to c$ transition, the modified currents up to $1/m_Q$ term are given by

$$\bar{c}\,\Gamma\, b = \bar{c}_{v'}\left(\Gamma-\frac{i\overleftarrow{D}_\mu}{2m_c}\gamma^\mu\Gamma+\Gamma\gamma^\mu\frac{iD_\mu}{2m_b}\right)b_v. \tag{C42}$$

Similarly to Eq. (C13), the above HQET operator is related to meson covariant fields as

$$\bar{c}_{v'}i\overleftarrow{D}_\mu\Gamma b_v = \mathrm{Tr}\left(\bar{H}_{v'}^{(c)}\Gamma H_v^{(b)}M_\mu(v,v')\right), \tag{C43}$$

$$\bar{c}_{v'}\Gamma iD_\mu b_v = -(\bar{b}_v i\overleftarrow{D}_\mu\bar{\Gamma}c_{v'})^\dagger = -\mathrm{Tr}\left(\bar{H}_{v'}^{(c)}\Gamma H_v^{(b)}M_\mu(v',v)\right). \tag{C44}$$

The most general form of $M_\mu(v,v')$ is expressed as

$$M_\mu(v,v') = \eta_+(v+v')_\mu+\eta_-(v-v')_\mu-\eta_3\gamma_\mu. \tag{C45}$$

Thus, $\bar{B}\to D^{(*)}$ transitions, which come from the flavor changing $b\to c$ current at the order of $1/m_Q$, are parametrized as the functions $\eta_{\pm,3}(w)$. The $1/m_Q$ corrections to the vector

form factors defined in Eqs. (B23), (B26) and (B27) are represented as,

$$\delta h_+^\eta = ((w+1)\eta_+ + (w-1)\eta_- + \eta_3)\left(\frac{1}{2m_c} + \frac{1}{2m_b}\right), \tag{C46}$$

$$\delta h_-^\eta = ((w+1)(\eta_+ + \eta_-) + 3\eta_3)\left(\frac{1}{2m_c} - \frac{1}{2m_b}\right), \tag{C47}$$

$$\delta h_V^\eta = -\eta_-\left(\frac{1}{m_c} + \frac{1}{m_b}\right) - \eta_3\left(\frac{1}{m_b}\right), \tag{C48}$$

$$\delta h_{A_1}^\eta = \eta_+\left(\frac{1}{m_c} + \frac{1}{m_b}\right) + \frac{\eta_3}{w+1}\left(\frac{1}{m_c} + \frac{2-w}{m_b}\right), \tag{C49}$$

$$\delta h_{A_2}^\eta = (\eta_+ + \eta_-)\left(\frac{1}{m_c}\right), \tag{C50}$$

$$\delta h_{A_3}^\eta = \eta_+\left(\frac{1}{m_c}\right) - (\eta_- + \eta_3)\left(\frac{1}{m_b}\right). \tag{C51}$$

There are another sources of $1/m_Q$ corrections, which come from the higher dimensional operators in the HQET Lagrangian:

$$\mathcal{L}^{(1)}_{\rm HQET} = -\bar{Q}_v \frac{D_\perp^2}{2m_Q} Q_v - g\bar{Q}_v \frac{\sigma_{\mu\nu}G^{\mu\nu}}{4m_Q} Q_v, \tag{C52}$$

which are given by expanding Eq. (C7). The first and second terms indicate the higher dimensional kinetic and chromomagnetic energy contributions respectively. These terms contribute to $\bar{B} \to D^{(*)}$ transitions in the following form:

$$\langle D^{(*)}| i\int d^4x\, T\left(-\bar{c}_{v'}\frac{D_\perp^2}{2m_c}c_{v'}\Big|_x\, \bar{c}_{v'}\Gamma b_v\Big|_0\right)|\bar{B}\rangle = -\frac{\chi_1}{m_c}\langle D^{(*)}|\,\mathrm{Tr}\left(\bar{H}^{(c)}_{v'}\frac{1+\not{v}'}{2}\Gamma H^{(b)}_v\right)|\bar{B}\rangle\,, \tag{C53}$$

$$\langle D^{(*)}| i\int d^4x\, T\left(-\bar{c}_{v'}\Gamma b_v\Big|_x\, \bar{b}_v\frac{D_\perp^2}{2m_b}b_v\Big|_0\right)|\bar{B}\rangle = -\frac{\chi_1}{m_b}\langle D^{(*)}|\,\mathrm{Tr}\left(\bar{H}^{(c)}_{v'}\Gamma\frac{1+\not{v}}{2}H^{(b)}_v\right)|\bar{B}\rangle\,, \tag{C54}$$

$$\langle D^{(*)}| i\int d^4x\, T\left(-\bar{c}_{v'}g\frac{\sigma_{\mu\nu}G^{\mu\nu}}{4m_c}c_{v'}\Big|_x\, \bar{c}_{v'}\Gamma b_v\Big|_0\right)|\bar{B}\rangle = \frac{1}{2m_c}\langle D^{(*)}|\,\mathrm{Tr}\left(X_{\mu\nu}\bar{H}^{(c)}_{v'}\sigma^{\mu\nu}\frac{1+\not{v}'}{2}\Gamma H^{(b)}_v\right)|\bar{B}\rangle\,, \tag{C55}$$

$$\langle D^{(*)}| i\int d^4x\, T\left(-\bar{c}_{v'}\Gamma b_v\Big|_x\, \bar{b}_v g\frac{\sigma_{\mu\nu}G^{\mu\nu}}{4m_b}b_v\Big|_0\right)|\bar{B}\rangle = \frac{1}{2m_b}\langle D^{(*)}|\,\mathrm{Tr}\left(X'_{\mu\nu}\bar{H}^{(c)}_{v'}\Gamma\frac{1+\not{v}}{2}\sigma^{\mu\nu}H^{(b)}_v\right)|\bar{B}\rangle\,, \tag{C56}$$

where the general forms of $X^{(\prime)}_{\mu\nu}$ are defined as

$$X_{\mu\nu} = 2\chi_2(v_\mu\gamma_\nu - v_\nu\gamma_\mu) + i4\chi_3\sigma_{\mu\nu}, \tag{C57}$$

$$X'_{\mu\nu} = 2\chi_2(v'_\mu\gamma_\nu - v'_\nu\gamma_\mu) + i4\chi_3\sigma_{\mu\nu}, \tag{C58}$$

and χ_i are the functions of w. Thus, $\bar{B} \to D^{(*)}$ transitions, which come from the HQET Lagrangian at the order of $1/m_Q$, are parametrized as the functions $\chi_{1,2,3}(w)$. The $1/m_Q$

corrections to the vector form factors are represented as,

$$\delta h_+^\chi = \chi_1 \left(\frac{1}{m_c} + \frac{1}{m_b}\right) - 2\left((w-1)\chi_2 - 3\chi_3\right)\left(\frac{1}{m_c} + \frac{1}{m_b}\right), \tag{C59}$$

$$\delta h_-^\chi = 0, \tag{C60}$$

$$\delta h_V^\chi = \chi_1 \left(\frac{1}{m_c} + \frac{1}{m_b}\right) - 2\chi_3 \left(\frac{1}{m_c}\right) - 2\left((w-1)\chi_2 - 3\chi_3\right)\left(\frac{1}{m_b}\right), \tag{C61}$$

$$\delta h_{A_1}^\chi = \chi_1 \left(\frac{1}{m_c} + \frac{1}{m_b}\right) - 2\chi_3 \left(\frac{1}{m_c}\right) - 2\left((w-1)\chi_2 - 3\chi_3\right)\left(\frac{1}{m_b}\right), \tag{C62}$$

$$\delta h_{A_2}^\chi = 2\chi_2 \left(\frac{1}{m_c}\right), \tag{C63}$$

$$\delta h_{A_3}^\chi = \chi_1 \left(\frac{1}{m_c} + \frac{1}{m_b}\right) - 2(\chi_2 + \chi_3)\left(\frac{1}{m_c}\right) - 2\left((w-1)\chi_2 - 3\chi_3\right)\left(\frac{1}{m_b}\right). \tag{C64}$$

While the $1/m_Q$ corrections to the $\bar{B} \to D^{(*)}$ form factors are parametrized as six undetermined functions in general as seen above, several functions relate to each other and one can reduce six functions to three independent functions. By use of the equation of motion, $(iv' \cdot D)c_{v'} = 0$, the undetermined functions $\eta_{\pm,3}$ relate to each other:

$$\eta_+(w)(w+1) + \eta_-(w)(w-1) + \eta_3(w) = 0. \tag{C65}$$

The $1/m_Q$ expansion is also applied to a expression of a meson mass by means of a heavy quark mass in the HQET. The meson mass M, containing heavy quark with its mass m_Q, is represented as

$$M = m_Q + \bar{\Lambda} + O\left(1/m_Q\right), \tag{C66}$$

where $\bar{\Lambda}$ indicates the contribution at the order of $(1/m_Q)^0$ term in $1/m_Q$ expansion, and thus $\bar{\Lambda}$ does not depend on heavy quark mass and flavor. In terms of $\bar{\Lambda}$ and the Isgur-Wise function $\xi(w)$, the function $\eta_-(w)$ can be represented as

$$\eta_-(w) = -\frac{1}{2}\bar{\Lambda}\xi(w). \tag{C67}$$

This equation is derived from the following relation:

$$i\partial_\mu\left(\bar{c}_{v'}\Gamma b_v\right) = \bar{\Lambda}(v_\mu - v'_\mu)\bar{c}_{v'}\Gamma b_v, \tag{C68}$$

$$= \bar{c}_{v'} i\overleftarrow{D}_\mu \Gamma b_v + \bar{c}_{v'}\Gamma i D_\mu b_v. \tag{C69}$$

The corrections $\delta h_+^\eta, \delta h_V^\eta, \delta h_{A_1}^\eta$ and $\delta h_{A_3}^\eta$ have the same contributions in the χ_1 term, which come from higher dimensional kinetic energy term, while $h_+^\eta = h_V^\eta = h_{A_1}^\eta = h_{A_3}^\eta = \xi(w)$ in

the HQL. Thus, we can effectively vanish χ_1 contribution by redefining Isgur-Wise function as

$$\xi + \chi_1 \left(\frac{1}{m_c} + \frac{1}{m_b} \right) \to \xi. \tag{C70}$$

As a consequence, the relevant $1/m_Q$ corrections to the $\bar{B} \to D^{(*)}$ form factors are rewritten and summarized as,

$$\delta h_+ = -2\left((w-1)\chi_2 - 3\chi_3\right)\left(\frac{1}{m_c} + \frac{1}{m_b}\right), \tag{C71}$$

$$\delta h_- = -\left(\frac{\bar{\Lambda}}{2}\xi - \eta_3\right)\left(\frac{1}{m_c} - \frac{1}{m_b}\right), \tag{C72}$$

$$\delta h_V = \left(\frac{\bar{\Lambda}}{2}\xi - 2\chi_3\right)\left(\frac{1}{m_c}\right) - \left(\eta_3 + 2(w-1)\chi_2 - 6\chi_3\right)\left(\frac{1}{m_b}\right), \tag{C73}$$

$$\begin{aligned}\delta h_{A_1} = &\left(\frac{w-1}{w+1}\frac{\bar{\Lambda}}{2}\xi - 2\chi_3\right)\left(\frac{1}{m_c}\right) \\ &+ \left(\frac{w-1}{w+1}(\frac{1}{2}\bar{\Lambda}\xi - \eta_3) - 2(w-1)\chi_2 + 6\chi_3\right)\left(\frac{1}{m_b}\right),\end{aligned} \tag{C74}$$

$$\delta h_{A_2} = -\frac{1}{w+1}\left(\bar{\Lambda}\xi + \eta_3 - 2(w+1)\chi_2\right)\left(\frac{1}{m_c}\right), \tag{C75}$$

$$\begin{aligned}\delta h_{A_3} = &\left(\frac{1}{w+1}\left((w-1)\frac{\bar{\Lambda}}{2}\xi - \eta_3\right) - 2(\chi_2 + \chi_3)\right)\left(\frac{1}{m_c}\right) \\ &+ \left(\frac{\bar{\Lambda}}{2}\xi - \eta_3 - 2(w-1)\chi_2 + 6\chi_3\right)\left(\frac{1}{m_b}\right),\end{aligned} \tag{C76}$$

by using the sub-leading Isgur-Wise functions, $\chi_{2,3}, \eta_3$ and $\bar{\Lambda}$. According to QCD sum rules, one predict $\bar{\Lambda} = 0.50 \pm 0.07\text{GeV}$ [65] and the approximate expressions for these functions are obtained, using QCD sum rules [66], as

$$\eta_3/\xi \simeq 0.62\bar{\Lambda}, \tag{C77}$$

$$\chi_2/\xi \simeq -0.06\bar{\Lambda}, \tag{C78}$$

$$\chi_3/\xi \simeq 0.04(w-1)\bar{\Lambda}. \tag{C79}$$

6. Summary

To summarize, the final expressions for the form factors including α_s and $1/m_Q$ corrections are represented as

$$h_+/\hat{\xi} = \hat{C}_1^V - \frac{w+1}{2}(\hat{C}_2^V + \hat{C}_3^V) + \hat{D}_+\left(\frac{\bar{\Lambda}}{m_c} + \frac{\bar{\Lambda}}{m_b}\right), \tag{C80}$$

$$h_-/\hat{\xi} = \frac{w+1}{2}(\hat{C}_3^V - \hat{C}_2^V) + \hat{D}_-\left(\frac{\bar{\Lambda}}{m_c} - \frac{\bar{\Lambda}}{m_b}\right), \tag{C81}$$

$$h_V/\hat{\xi} = \hat{C}_1^V + \hat{D}_V^1\left(\frac{\bar{\Lambda}}{m_c}\right) + \hat{D}_V^2\left(\frac{\bar{\Lambda}}{m_b}\right), \tag{C82}$$

$$h_{A_1}/\hat{\xi} = \hat{C}_1^A + \hat{D}_{A_1}^1\left(\frac{\bar{\Lambda}}{m_c}\right) + \hat{D}_{A_1}^2\left(\frac{\bar{\Lambda}}{m_b}\right), \tag{C83}$$

$$h_{A_2}/\hat{\xi} = \hat{C}_2^A + \hat{D}_{A_2}\left(\frac{\bar{\Lambda}}{m_c}\right), \tag{C84}$$

$$h_{A_3}/\hat{\xi} = \hat{C}_1^A - \hat{C}_3^A + \hat{D}_{A_3}^1\left(\frac{\bar{\Lambda}}{m_c}\right) + \hat{D}_{A_3}^2\left(\frac{\bar{\Lambda}}{m_b}\right), \tag{C85}$$

where $\hat{C}_i^{V/A}$ are shown in Eqs. (C38)–(C40) and $\hat{D}_i$ are approximately represented as $\hat{D}_+ \simeq 0.36(w-1)$, $\hat{D}_- \simeq -0.08(w-1)$, $\hat{D}_V^1 \simeq 0.5 - 0.08(w-1)$, $\hat{D}_V^2 \simeq -0.12 + 0.36(w-1)$, $\hat{D}_{A_1}^1 \simeq 0.17(w-1)$, $\hat{D}_{A_1}^2 \simeq 0.60(w-1)$, $\hat{D}_{A_2} \simeq -0.93 + 0.41(w-1)$, $\hat{D}_{A_3}^1 \simeq -0.19 + 0.33(w-1)$, $\hat{D}_{A_3}^2 \simeq -0.12 + 0.36(w-1)$.

APPENDIX D: HADRONIC AMPLITUDES

1. Expressions

Using the definitions as shown in appendix B, the hadronic amplitudes given in Eqs. (36) and (37) are represented as

$$H^s_{V_1,\pm} = H^s_{V_2,\pm} = 0\,, \tag{D1}$$

$$H^s_{V_1,0} = H^s_{V_2,0} = m_B\sqrt{r}\frac{\sqrt{w^2-1}}{\sqrt{\hat{q}^2(w)}}\left[(1+r)h_+(w) - (1-r)h_-(w)\right]\,, \tag{D2}$$

$$H^s_{V_1,s} = H^s_{V_2,s} = m_B\sqrt{r}\frac{1}{\sqrt{\hat{q}^2(w)}}\left[(1-r)(w+1)h_+(w) - (1+r)(w-1)h_-(w)\right]\,, \tag{D3}$$

$$\begin{aligned} H^{\pm}_{V_1,\pm} &= -H^{\mp}_{V_2,\mp} \\ &= m_B\sqrt{r}\left[(w+1)h_{A_1}(w) \mp \sqrt{w^2-1}h_V(w)\right]\,, \end{aligned} \tag{D4}$$

$$\begin{aligned} H^0_{V_1,0} &= -H^0_{V_2,0} \\ &= m_B\sqrt{r}\frac{w+1}{\sqrt{\hat{q}^2(w)}}\left[-(w-r)h_{A_1}(w) + (w-1)(rh_{A_2}(w) + h_{A_3}(w))\right], \end{aligned} \tag{D5}$$

$$\begin{aligned} H^0_{V_1,s} &= -H^0_{V_2,s} \\ &= m_B\sqrt{r}\frac{\sqrt{w^2-1}}{\sqrt{\hat{q}^2(w)}}\left[-(w+1)h_{A_1}(w) + (1-rw)h_{A_2}(w) + (w-r)h_{A_3}(w)\right], \end{aligned} \tag{D6}$$

and others = 0. In the heavy quark limit, we obtain $h_+(w) = h_{A_{1,3}}(w) = h_V(w) = \xi(w)$ and $h_-(w) = h_{A_2}(w) = 0$.

For the scalar and pseudo-scalar operators, the hadronic amplitudes in Eqs. (38) and (39) are represented as

$$H^s_{S_1} = H^s_{S_2} = m_B\sqrt{r}(w+1)h_S(w)\,, \tag{D7}$$

$$H^{\pm}_{S_1} = H^{\pm}_{S_2} = 0\,, \tag{D8}$$

$$H^0_{S_1} = -H^0_{S_2} = -m_B\sqrt{r}\sqrt{w^2-1}\,h_P(w)\,. \tag{D9}$$

For the tensor operator, the hadronic amplitudes in Eq. (40) are represented as

$$H^s_{+-}(q^2) = H^s_{0s}(q^2) = -m_B\sqrt{r}\sqrt{w^2-1}\,h_T(w)\,, \tag{D10}$$

$$\begin{aligned} H^{\pm}_{\pm 0}(q^2) &= \pm H^{\pm}_{\pm s}(q^2) \\ &= \pm m_B\sqrt{r}\frac{1-rw\pm r\sqrt{w^2-1}}{\sqrt{\hat{q}^2(w)}} \\ &\quad\times\left[h_{T_1}(w)+h_{T_2}(w)+(w\pm\sqrt{w^2-1})(h_{T_1}(w)-h_{T_2}(w))\right]\,, \end{aligned} \tag{D11}$$

$$\begin{aligned} H^0_{+-}(q^2) &= H^0_{0s}(q^2) \\ &= -m_B\sqrt{r}\left[(w+1)h_{T_1}(w)+(w-1)h_{T_2}(w)+2(w^2-1)h_{T_3}(w)\right]\,, \end{aligned} \tag{D12}$$

and the rest is obtained by $H^{\lambda_M}_{\lambda\lambda'}(q^2) = -H^{\lambda_M}_{\lambda'\lambda}(q^2)$ and others $= 0$.

2. Redefinitions of vector types form factors

We obtain the expressions for the vector types form factors using the HQET in appendix C. The remaining unknown function is the leading Isgur-Wise function $\xi(w)$. In order to evaluate this function by using dispersion relations, it is convenient to redefine the form factors as follow [34]:

$$V_1(w) = h_+(w) - \frac{1-r}{1+r}h_-(w)\,, \tag{D13}$$

$$S_1(w) = h_+(w) - \frac{1+r}{1-r}\frac{w-1}{w+1}h_-(w)\,, \tag{D14}$$

$$A_1(w) = h_{A_1}(w)\,, \tag{D15}$$

$$R_1(w) = \frac{h_V(w)}{h_{A_1}(w)}\,, \tag{D16}$$

$$R_2(w) = \frac{h_{A_3}(w)+rh_{A_2}(w)}{h_{A_1}(w)}\,, \tag{D17}$$

$$R_3(w) = \frac{h_{A_3}(w)-rh_{A_2}(w)}{h_{A_1}(w)}\,. \tag{D18}$$

According to Ref.[34], $V_1(w)$ and $A_1(w)$ are parametrized as in Eqs. (65) and (66) respectively. For $S_1(w)$ and $R_i(w)$, we estimate [27]

$$S_1(w)/V_1(w) = 0.981 + 0.041(w-1) - 0.015(w-1)^2, \tag{D19}$$

$$R_1(w) = 1.40 - 0.12(w-1) + 0.05(w-1)^2, \tag{D20}$$

$$R_2(w) = 0.85 + 0.11(w-1) - 0.06(w-1)^2, \tag{D21}$$

$$R_3(w) = 1.22 - 0.052(w-1) + 0.026(w-1)^2, \tag{D22}$$

by using the modified form factors including HQET corrections as shown in the previous appendix.

3. Evaluations for scalar and tensor types form factors

In order to evaluate the amplitudes in the case of scalar or tensor type interaction, we have to valuate the form factors defined above. For naive estimation, it is useful to take into account the equations of motion in the quark currents, that result in

$$i\partial_\mu \left(\bar{c}\gamma^\mu b\right) = \left(m_b - m_c\right)\bar{c}b\,, \tag{D23}$$

$$i\partial_\mu \left(\bar{c}\gamma^\mu\gamma^5 b\right) = -\left(m_b + m_c\right)\bar{c}\gamma^5 b, \tag{D24}$$

$$\partial_\mu \left(\bar{c}\sigma^{\mu\nu} b\right) = -\left(m_b + m_c\right)\bar{c}\gamma^\nu b - \left(i\partial^\nu \bar{c}\right) b + \bar{c}\left(i\partial^\nu b\right), \tag{D25}$$

which lead to the following relations among form factors:

$$\begin{aligned} h_S(w) &= h_+(w) - \frac{1+r}{1-r}\frac{w-1}{w+1}h_-(w) + O\left(\frac{\bar{\Lambda}^2}{m_Q^2}\right) \\ &= S_1(w) + O\left(\frac{\bar{\Lambda}^2}{m_Q^2}\right), \end{aligned} \tag{D26}$$

$$\begin{aligned} h_P(w) &= \frac{1}{1+r}\left[(w+1)h_{A_1}(w) + (rw-1)h_{A_2}(w) - (w-r)h_{A_3}(w)\right] + O\left(\frac{\bar{\Lambda}}{m_Q}\right) \\ &= \frac{A_1(w)}{1+r}\left[w+1 - \frac{1-r^2}{2r}R_2(w) + \frac{\hat{q}^2(w)}{2r}R_3(w)\right] + O\left(\frac{\bar{\Lambda}}{m_Q}\right), \end{aligned} \tag{D27}$$

$$h_T(w) = h_+(w) - \frac{1+r}{1-r}h_-(w) + O\left(\frac{\bar{\Lambda}}{m_Q}\right), \tag{D28}$$

$$h_{T_1}(w) = \frac{1}{2\hat{q}^2(w)}\left[(1-r)^2(w+1)h_{A_1}(w) - (1+r)^2(w-1)h_V(w)\right] + O\left(\frac{\bar{\Lambda}}{m_Q}\right), \tag{D29}$$

$$h_{T_2}(w) = \frac{(1-r^2)(w+1)}{2\hat{q}^2(w)}\left[h_{A_1}(w) - h_V(w)\right] + O\left(\frac{\bar{\Lambda}}{m_Q}\right), \tag{D30}$$

$$\begin{aligned} h_{T_3}(w) = -\frac{1}{2(1+r)\hat{q}^2(w)}&\left[2r(w+1)h_{A_1}(w) - \hat{q}^2(w)\left(rh_{A_2}(w) - h_{A_3}(w)\right)\right. \\ &\left. -(1+r)^2 h_V(w)\right] + O\left(\frac{\bar{\Lambda}}{m_Q}\right). \end{aligned} \tag{D31}$$

where we have used $m_{B(M)} = m_{b(c)} + \bar{\Lambda} + O\left(\bar{\Lambda}^2/m_{b(c)}\right)$. The absence of $1/m_Q$ corrections in Eq. (D26) is confirmed by the heavy quark expansion without resort to the equations of motion. Thus we employ $h_S(w) = S_1(w) = \left[1 + \Delta(w)\right] V_1(w)$, where $\Delta(w)$ involves the $1/m_Q$ corrections. On the other hand, there exist unknown $1/m_Q$ corrections in Eq. (D27).

We ignore them, but use the axial vector form factors $A_1(w)$ and $R_{2,3}(w)$ including $1/m_Q$ corrections as described in Sec. II. Similarly to the case of the scalar type form factors, we ignore the unknown $1/m_Q$ corrections in the tensor type form factors, and employ the vector and axial vector form factors with the $1/m_Q$ corrections.

---

[1] For instance, R. E. Marshak, Riazuddin and C. P. Ryan, *THEORY OF WEAK INTERACTIONS*, John Wiley & Sons (1969).

[2] For a review, *e.g.*, J. F. Gunion, H. E. Haber, G. Kane and S. Dawson, *The Higgs Hunter's Guide*, Frontiers in Physics series, Addison-Wesley (1990).

[3] See, *e.g.* H. P. Nilles, Phys. Rept. **110**, 1 (1984); S. P. Martin, *A Supersymmetry Primer*, in *Perspectives on Supersymmetry II*, G.L. Kane (ed.), World Scientific (2010). hep-ph/9709356.

[4] B. Grzadkowski and W. S. Hou, Phys. Lett. B **283**, 427 (1992).

[5] W. S. Hou, Phys. Rev. D **48**, 2342 (1993).

[6] I. Adachi *et al.* (Belle Collaboration), arXiv:1208.4678 [hep-ex].

[7] J. P. Lees et al., Phys. Rev. Lett. **109**, 101802 (2012). arXiv:1205.5442 [hep-ex].

[8] H. Na, C. Monahan, C. T. H. Davies, R. Horgan, G. P. Lepage, and J. Shigemitsu, Phys. Rev. D**86**,034506 (2012).

[9] B. Aubert *et al.* (BABAR Collaboration), Phys. Rev. D **81**, 051101(R) (2010). arXiv:0809.4027 [hep-ex].

[10] J. Beringer *et al.* (Particle Data Group), Phys. Rev. D **86**, 010001 (2012).

[11] M. Neubert, Phys. Rep. **245**, 259 (1994). hep-ph/9306320.

[12] A. Matyja *et al.* (Belle Collaboration), Phys. Rev. Lett. **99**(2007)191807. arXiv:0706.4429 [hep-ex].

[13] I. Adachi *et al.* (Belle Collaboration), arXiv:0910.4301 [hep-ex].

[14] A. Bozek *et al.* (Belle Collaboration), Phys. Rev. D **82**, 072005 (2010). arXiv:1005.2302 [hep-ex].

[15] K. Kiers and A. Soni, Phys. Rev. D **56**, 5786 (1997). hep-ph/9706337.

[16] C.-H. Chen and C.-Q. Geng, Phys. Rev. D **71**, 077501 (2005). hep-ph/0503123.

[17] C.-H. Chen and C.-Q. Geng, JHEP 0610, **053**, 2006. hep-ph/0608166.

[18] U. Nierste, S. Trine and S. Westhoff, Phys. Rev. D **78**, 015006 (2008). arXiv:0801.4938 [hep-

ph].

[19] S. Trine, Talk given at 34th International Conference on High Energy Physics (ICHEP 2008), Philadelphia, Pennsylvania, 30 Jul - 5 Aug 2008. arXiv:0810.3633 [hep-ph].

[20] J. F. Kamenik and F. Mescia, Phys. Rev. D **78**, 014003 (2008). arXiv:0802.3790 [hep-ph].

[21] Y. Sakaki and H. Tanaka, arXiv:1205.4908 [hep-ph].

[22] D. Birevica, N. Kosnikb, and A. Tayduganov Phys. Lett. B**716**, 208 (2012). arXiv:1206.4977 [hep-ph].

[23] J. A. Bailey, *et al.*, Phys. Rev. Lett. **109**, 071802 (2012). arXiv:1206.4992 [hep-ph].

[24] A. Celis, M. Jung, X.-Q. Li, and A. Pich, arXiv:1210.8443 [hep-ph].

[25] S. Fajfer, J. F. Kamenik and I. Nišandžić, Phys. Rev. D **85**, 094025 (2012). arXiv:1203.2654 [hep-ph].

[26] A. Datta, M. Duraisamy, and D. Ghosh, Phys. Rev. D**86**, 034027 (2012). arXiv:1206.3760 [hep-ph].

[27] M. Tanaka and R. Watanabe, arXiv:1212.1878.

[28] M. Tanaka, Z. Phys. C **47**, 321 (1995). hep-ph/9411405.

[29] M. Tanaka and R. Watanabe, Phys. Rev. D **82**, 034027 (2010).

[30] K. Hagiwara, A.D. Martin, and M.F. Wade, Nucl. Phys. **B327**, 569 (1989).

[31] K. Hagiwara, A.D. Martin, and M.F. Wade, Z. Phys. **C46**, 299 (1990).

[32] N. Isgur and M.B. Wise, Phys. Lett **B232**, 113 (1989); Phys. Lett **B237**, 527 (1990).

[33] M. E. Luke, Phys. Lett. **252**, 447 (1990).

[34] I. Caprini, L. Lellouch, and M. Neubert, Nucl. Phys. **B530**, 153 (1998). hep-ph/9712417.

[35] The Heavy Flavor Averaging Group, `http://www.slac.stanford.edu/xorg/hfag/`, 2011.

[36] R. Kowalewski and T. Mannel, "*Determination of Vcb and Vub*," in PDG review.

[37] E. Gamiz, C. T. H. Davies, G. P. Lepage, J. Shigemitsu and M. Wingate (HPQCD Collaboration), Phys. Rev. D **80**, 014503 (2009).

[38] Y. Amhis (The Heavy Flavor Averaging Group), arXiv:1207.1158[hep-ex].

[39] W. Altmannshofer, P. Paradisi and D. M. Straub, JHEP 04, 008 (2012)

[40] S. Fajfer, J. F. Kamenik, I. Nišandžić and J. Zupan, Phys. Rev. Lett. **109**, 161801 (2012). arXiv:1206.1872 [hep-ph].

[41] A. Crivellin, C. Greub, and A. Kokulu, Phys. Rev. D**86**, 054014 (2012). arXiv:1206.2634 [hep-ph].

[42] A. Rougé, in the proceedings of *the Workshop on Tau Lepton Physics*, Orsay (1990), eds. M. Davier and B. Jean-Marie (Editions Frontières, 1991) p. 213. FPRINT-91-06, 1991.

[43] M. Davier, L. Duflot, F. Le Diberder, and A. Rouge, Phys. Lett. B**306**, 411, 1993.

[44] T. Aushev *et al.*, arXiv:1002.5012 [hep-ex]

[45] V. D. Barger, J. L. Hewett, and R. J. N. Phillips, Phys. Rev. D **41**, 3421 (1990).

[46] Y. Grossman, Nucl. Phys. B **426**, 355 (1994).

[47] A. G. Akeroyd and W. J. Stirling, Nucl. Phys. B **447**, 3 (1995); A. G. Akeroyd, Phys. Lett. B **377**, 95 (1996); J. Phys. G **24**, 1983 (1998).

[48] M. Aoki, S. Kanemura, K. Tsumura, and K. Yagyu, Phys. Rev. D **80**, 015017, 2009.

[49] G. Aad *et al.* (ATLAS Collaboration), Phys. Lett. B**716**, 1 (2012).

[50] S. Chatrchyan *et al.* (CMS Collaboration), Phys. Lett. B**716**, 30 (2012).

[51] H. Itoh, S. Komine and Y. Okada, Prog. Theor. Phys. **114**, 179, 2005. hep-ph/0409228.

[52] A. Crivellin, Phys. Rev. D **83**, 056001 (2011).

[53] R. Barbier *et al.*, Phys. Rep. **420**, 1 (2005).

[54] G.-C. Cho, H. Matsuo, Phys. Lett. B**703**, 318 (2011).

[55] N. G. Deshpande, and A. Menon, arXiv:1208.4134 [hep-ph].

[56] J. Erler, J. L. Feng, and N. Polonsky, Phys. Rev. Lett. **78**, 3063 (1997).

[57] M. Chemtob, Prog. Part. Nucl. Phys. **54**, 71 (2005).

[58] Y. Grossman, Z. Ligeti, and E. Nardi, Nucl. Phys. **B465**, 369 (1996), Nuclear Phys. **B480**, 753 (1996).

[59] W. Altmannshofer, A. J. Buras, D. M. Straub, and M. Wick, JHEP **04**, 022 (2009).

[60] R. Barate *et al.* (ALEPH Collaboration), Eur. Phys. J. C **19**, 213 (2001).

[61] Y. Sakaki, M. Tanaka. A. Tayduganov, and R. Watanabe, in preparation.

[62] W. Buchmuller, R. Ruckl, and D. Wyler, Phys. Lett. B**191**, 442 (1987); Phys. Lett. B**448**, 320(E) (1999).

[63] J. P. Lee, Phys. Lett. B **526**, 61 (2002).

[64] T. Miki, T. Miura and M. Tanaka, hep-ph/0210051.

[65] M. Neubert, Phys. Rev. D**46**, 1076 (1992).

[66] M. Neubert, Z. Ligeti and Y. Nir, Phys. Lett. B**301**, 101 (1993); Phys. Rev. D**47**, 5060 (1993); Phys. Rev. D**49**, 1301 (1994).

[67] A. Crivellin, Phys. Rev. D **81**, 031301 (2010)